



This discussion paper is/has been under review for the journal Atmospheric Chemistry and Physics (ACP). Please refer to the corresponding final paper in ACP if available.

Source contributions to 2012 summertime aerosols in the Euro-Mediterranean region

G. Rea¹, S. Turquety¹, L. Menut¹, R. Briant¹, S. Mailler¹, and G. Siour²

¹Laboratoire de Météorologie Dynamique, UMR CNRS 8539, Université Pierre et Marie Curie – Paris 6, ENPC, Ecole Polytechnique, Palaiseau, France

²Laboratoire Inter-Universitaire des Systèmes Atmosphériques, UMR CNRS 7583, Université Paris Est Créteil et Université Paris Diderot, Institut Pierre Simon Laplace, Créteil, France

Received: 2 February 2015 – Accepted: 6 March 2015 – Published: 18 March 2015

Correspondence to: G. Rea (geraldine.rea@lmd.polytechnique.fr)

Published by Copernicus Publications on behalf of the European Geosciences Union.

Title Page

Abstract

Introduction

Conclusions

References

Tables

Figures



Back

Close

Full Screen / Esc

Printer-friendly Version

Interactive Discussion



Abstract

In the Mediterranean area, aerosols may originate from anthropogenic or natural emissions (biogenic, mineral dust, fire and sea salt) before undergoing complex chemistry. In case of a huge pollution event, it is important to know if European pollution limits are exceeded and, if yes, if the pollution is due to anthropogenic or natural sources. In this study, the relative contribution of emissions to surface PM₁₀, surface PM_{2.5} and total aerosol optical depth (AOD) is quantified. For Europe and the Mediterranean regions and during the summer of 2012, the WRF and CHIMERE models are used to perform a sensitivity analysis: one simulation with all sources (reference) and all others with one source removed. The reference simulation is compared to data from the AirBase and AERONET networks and the MODIS satellite instrument to quantify the ability of the model to reproduce the observations. It is shown that the correlation ranges from 0.38 to 0.49 for surface particulate matter and from 0.35 to 0.75 for AOD. The sensitivity simulations are analysed to quantify the impact of each source. For the summer of 2012, the model shows that the region (from -10° W to 40° E and from 30 to 55° N) is mainly influenced by aerosols due to mineral dust and anthropogenic emissions (62 and 19 % respectively of total surface PM₁₀ and 17 and 52 % of total surface PM_{2.5}). The western part of the Mediterranean is strongly influenced by mineral dust emissions (86 % for surface PM₁₀ and 44 % for PM_{2.5}), while anthropogenic emissions dominate in the northern Mediterranean basin (up to 75 % for PM_{2.5}). Fire emissions are more sporadic but may represent 20 % of surface PM_{2.5} near local sources. Sea salt mainly contribute for coastal sites (up to 29 %) and biogenic emissions mainly in Central Europe (up to 20 %).

The same analysis was undertaken for the number of stations in daily exceedances of the European Union limit of 50 µg m⁻³ for PM₁₀ (over the AirBase stations). This number is generally overestimated by the model, particularly in the northern part of the domain, but exceedances are captured at the right time. The discrepancies are most probably due to an overestimation of dust at the surface, and particularly when diverse

ACPD

15, 8191–8242, 2015

Contributions to 2012 summertime aerosols in the Euro-Mediterranean region

G. Rea et al.

Title Page

Abstract

Introduction

Conclusions

References

Tables

Figures

◀

▶

◀

▶

Back

Close

Full Screen / Esc

Printer-friendly Version

Interactive Discussion

Contributions to 2012 summertime aerosols in the Euro-Mediterranean region

G. Rea et al.

Title Page

Abstract

Introduction

Conclusions

References

Tables

Figures

◀

▶

◀

▶

Back

Close

Full Screen / Esc

Printer-friendly Version

Interactive Discussion



belt and the mid-latitude westerlies and low pressure systems, the Mediterranean region is characterized by hot, dry summers and mild, wet winters. These meteorological patterns govern the transport of aerosols released from various sources around the Mediterranean region and lead to a maximum aerosol load during the summer (Monks et al., 2009; Nabat et al., 2013). Moreover, a mixture of different sources is usually observed due to the long-range transport of the associated particles (Dall'Osto et al., 2010; Gerasopoulos et al., 2011; Boselli et al., 2012). Due to these complex characteristics, the specific impact of each aerosol source cannot be easily assessed.

The region is impacted by local emissions from anthropogenic activities and by biogenic emissions of precursors of aerosol formation. Most of $PM_{2.5}$ exceedances are due to primary pollution but these are enhanced by the production of secondary aerosols (Koçak et al., 2007). For instance, Sartelet et al. (2012) found that Secondary Organic Aerosol (SOA) formation over Europe is strongly impacted by biogenic emissions (72–88 %) in addition to anthropogenic emissions of precursors.

Moreover, the long-range transport of mineral dust from North Africa significantly affects PM concentration throughout the region. Several studies of available observations show that the PM_{10} European Union air quality standard ($50 \mu g m^{-3}$, daily average) is exceeded at many location around the basin because of mineral dust in addition to local anthropogenic pollutants (Gerasopoulos et al., 2006; Gobbi et al., 2007; Koçak et al., 2007; Rodriguez et al., 2007; Kaskaoutis et al., 2008). Mineral dust outbreaks, although transported through the Mediterranean sea during all seasons, are more frequent in spring and summer, where dust plumes are transported through the Atlantic and reach mainly and regularly the western part of the region (Moulin et al., 1998; Israelevich et al., 2012; Salvador et al., 2014; Ripoll et al., 2015). In summer, mineral dust aerosols are also observed over central Europe (Israelevich et al., 2012; Salvador et al., 2014).

Another important source of PM in the Mediterranean basin is sea salt, which can account for instance in Erdemli (Eastern Mediterranean) for up to 50 % of PM_{10} pollution thresholds exceedances (Koçak et al., 2007).

and by several satellite-based instruments, allowing a very good spatial and temporal coverage.

In addition to the analysis of surface and remote sensing observations, chemistry-transport models (CTMs) are required for the simulation of atmospheric composition and the understanding of physico-chemical processes. Model validation or inter-comparisons have shown that, although the modelling of ozone or other gases has been improved in the past years, the modelling of PM is still a concern, with a persistent underestimation of PM₁₀ for the majority of the CTMs (Roustan et al., 2010; Solazzo et al., 2012). Moreover, PM_{2.5} is also overestimated when PM₁₀ is improved, although the biases on PM_{2.5} are lower than those on PM₁₀. Even though emissions probably constitute a significant source of uncertainty, the uncertainty in modelled PM concentrations linked to the parameterization choices (vertical diffusion, number of levels, deposition, etc.) and to the meteorological fields can be for instance higher than the uncertainty linked to PM anthropogenic and biogenic emissions (Sartelet et al., 2012).

This paper provides an analysis of the main contributions of aerosol sources to both surface PM and Aerosol Optical Depth (AOD) in the Mediterranean region using the state-of-the-art regional CTM CHIMERE (Menut et al., 2013). The majority of the studies previously cited have been made at specific experimental sites and sometimes for specific case studies. This paper aims at estimating the contribution of each source in Europe and the Mediterranean Basin, to provide a description of the zones of influence of given sources on regional air pollution.

After an evaluation of the model's performance through comparisons to observations from surface networks and remote sensing, a sensitivity analysis is conducted on the case study of the summer of 2012 (June-July-August). This time period allows an analysis including all sources (fires and dust outbreaks notably occurred during this period). Estimations of the relative contributions of the main aerosol sources to the aerosol load in the Mediterranean area is provided. Section 2 describes particulate pollution during the summer of 2012 based on the available observations of surface PM and AOD. Section 3 presents the tools and methodology used in this paper. The model is evaluated

Contributions to 2012 summertime aerosols in the Euro-Mediterranean region

G. Rea et al.

Title Page	
Abstract	Introduction
Conclusions	References
Tables	Figures
◀	▶
◀	▶
Back	Close
Full Screen / Esc	
Printer-friendly Version	
Interactive Discussion	



200 $\mu\text{g m}^{-3}$. The Po Valley and the Benelux are also affected by high levels (up to 200 $\mu\text{g m}^{-3}$) as well as Eastern Europe.

For example, high values of PM are detected in Farollilo near Salamanca, Spain (Fig. 2) at the end (27–28) of June (with a concentration up to 120 $\mu\text{g m}^{-3}$), and end of July and above 80 during August (around the 10 and 18–19). The level of PM in this area remains high (around 40 $\mu\text{g m}^{-3}$ for daily mean) during the whole time period. Observations in the South of France show lower temporal variability with concentrations from 10 to around 50 $\mu\text{g m}^{-3}$. Some sporadic hourly values (not shown) reach more than 100 $\mu\text{g m}^{-3}$ around the 20–21 June, at the end of July and the end of August. For example, at the station located in Miramas in South of France, hourly values reach more than 250 $\mu\text{g m}^{-3}$ (80 of the daily mean values) around the 20 June, during the end of July, and during the beginning of August.

Eastern Europe is also affected by high concentrations, as shown for example by the Lomza station in Poland, with peak values around the 30 June (up to 90 $\mu\text{g m}^{-3}$), at the end of July (above 300 $\mu\text{g m}^{-3}$ for Mragowo, Poland) and during the second half of August (up to 100 $\mu\text{g m}^{-3}$).

2.2 Aerosol optical depth (AOD)

In addition to surface PM, remote sensing observations of AOD, which provides information on the column integrated aerosol load, are analysed. Both surface remote sensing from AERONET and satellite observations from the Moderate Resolution Imaging Spectroradiometer (MODIS) are used.

AERONET is an optical ground-based aerosol-monitoring network, composed of spectral radiometers. It allows measurements of AOD every 15 min at 8 wavelengths (centred between 340 and 1020 nm). With more than one hundred stations in the world, the network is widely used for the validation of model simulations and satellites observations. The main product examined here is the total AOD at 500 nm from the level

Title Page

Abstract

Introduction

Conclusions

References

Tables

Figures

◀

▶

◀

▶

Back

Close

Full Screen / Esc

Printer-friendly Version

Interactive Discussion

2.0 cloud screened and quality assured retrievals of the ground based AERONET sun photometers.

The estimated precision of the direct AOD measurements is ~ 0.01 (at 440 nm) for a recently calibrated instrument (Holben et al., 1998), and the uncertainties are well-documented (Dubovik et al., 2000). During the period of the simulation and within the domain, data from 53 stations of the network are available. Their location is shown in Fig. 1.

Surface site measurements do not allow a full regional evaluation, particularly around the Mediterranean Basin, which is poorly covered. Satellite observations therefore offer a good complement. MODIS is carried on board the Terra and Aqua satellites (NASA) and enables a daily near-global coverage of the Earth with its large swath of almost 2330 km. The satellites cross the equator at about 10:30 and 13:30, local time (ascending node) respectively. The measurements over 36 spectral bands (from 0.41 to 15 μm) allow the retrieval of many aerosols properties. For this study, the aerosol products MOD04 (for Terra) and MYD04 (for Aqua) L2 5.2 collection data are used (Remer et al., 2006). It includes daily AOD at 550 nm, as well as the Deep-Blue AOD (Sayer et al., 2013) that provides AOD over bright land areas (especially useful here for North Africa). They are available at 10 km \times 10 km resolution. The expected error for the AOD is $\pm 0.05 \pm 0.15\tau$ over land and $\pm 0.03 \pm 0.05\tau$ over ocean, with a good agreement with ground based measurements (Remer et al., 2005).

Spatial patterns of AOD over the region are similar to the ones observed in terms of surface PM concentrations (Fig. 1, bottom right panel), with high values at the south of the domain (up to 2 for North Africa and all around the Mediterranean Sea on a seasonal average), the Po Valley and Northern Europe (up to 1.2). MODIS allows a better coverage than surface measurements in some regions, like North Africa, the Mediterranean Sea, the Atlantic Ocean, the Balkans and the eastern part of the domain (Eastern Europe, Middle East, etc.) For example, large values of AOD, from 1 to 2, are observed with MODIS in the Balkans.

Contributions to 2012 summertime aerosols in the Euro-Mediterranean region

G. Rea et al.

Title Page

Abstract

Introduction

Conclusions

References

Tables

Figures

◀

▶

◀

▶

Back

Close

Full Screen / Esc

Printer-friendly Version

Interactive Discussion



Contributions to 2012 summertime aerosols in the Euro-Mediterranean region

G. Rea et al.

Title Page

Abstract

Introduction

Conclusions

References

Tables

Figures

◀

▶

◀

▶

Back

Close

Full Screen / Esc

Printer-friendly Version

Interactive Discussion



Time series for three AERONET stations are shown in Fig. 3. Clear enhancements are detected above Granada at the end of June (19 and 25–26), and in August (2, 8–9 and 18). The Timisoara station shows values around 1 on the 24 of August for both MODIS and AERONET. Finally, observations at Belsk in Poland show lower values but a notable peak around 1 July.

A comparison of these AOD observations for 2012 against the climatology from Nabat et al. (2013), which includes the AOD from 2003 to 2009 using both model and satellite-derived AOD products, indicates that this summer was in the average regarding the aerosol load. Exceptions appears in June where the AOD was higher than the climatology in North Africa and over the Atlantic Ocean near North African coasts, and in August with high values over the Balkans and over the Mediterranean close to the Spanish coastline. There are also higher punctual values in Spain in July. This comparison shows that the period was affected by air pollution from different sporadic events.

From this analysis, several regions and time periods with enhanced aerosol concentrations are identified during the summer of 2012. North Africa and the western Mediterranean Basin were regularly affected by the highest aerosol loads, with extreme peaks around 26 June and three times in August (daily mean of around $130 \mu\text{g m}^{-3}$ for PM_{10} and AOD around 1). Eastern Europe appears to show other influences with high concentrations of surface PM at the end of June, the end of July and the end of August (daily mean of $40 \mu\text{g m}^{-3}$ for PM_{10} , AOD up to 0.8). In the Balkans, MODIS also observed relatively high AOD (around 1) at the end of August.

For the rest of this study, the domain was divided into six sub-regions, which present different characteristics in terms of sources, population density as well as meteorological patterns, which are reflected in the observations. The acronym MED and NEU represent respectively all the Mediterranean Basin and the northern European part of the domain. MED and NEU regions are divided into western, central and eastern zones (MED-We, MED-Ce, MED-Ea and NEU-We, NEU-Ce, NEU-Ea). The delimitation of the regions are indicated in Table 1 and Fig. 1.

3 Modelling tools

The sensitivity of aerosol concentrations in the region to each source is evaluated using the CHIMERE regional CTM, driven by meteorological simulations performed using the mesoscale non-hydrostatic Weather Research and Forecasting (WRF) model.

The analysis is focused on the summer of 2012 (1 June to 31 August), with a 10 d spin-up. The simulation domain is chosen to include all contributing sources around the basin (including North Africa until Sahel, a part of the Atlantic Ocean, eastern and northern Europe). A Lambert conformal projection is used with a constant horizontal resolution of 50 km × 50 km. The domain is represented on Fig. 4.

This section introduces the models used, their configuration for this analysis, the emissions databases as well as the numerical approach used.

3.1 The WRF meteorological model

The meteorological fields are simulated using the WRF model version 3.5.1 (Skamarock et al., 2008), on a 50 km horizontal grid (same horizontal domain described above). The simulation has been performed with boundary conditions and nudging from the meteorological analysis data of NCEP (Kalnay et al., 1996), provided on a regular 1.125° × 1.125° grid.

The model is used in its non-hydrostatic configuration. The vertical grid covers 30 levels from the surface to 50 hPa. The WRF Single-Moment 6-class (Hong and Lim, 2006) is used for microphysics, and RRTMG (Iacono et al., 2008) and the Dudhia schemes (Dudhia, 1989) are used for long and short wave radiation respectively. The surface planetary boundary layer physics use the Noah Land Surface Model and Yonsei University scheme and the cumulus parameterization is based on the Kain–Fritsch scheme (Kain, 1993).

The WRF simulation outputs are then interpolated on the vertical resolution of CHIMERE and used to diagnose additional parameters (e.g. boundary layer height,

Contributions to 2012 summertime aerosols in the Euro-Mediterranean region

G. Rea et al.

Title Page

Abstract

Introduction

Conclusions

References

Tables

Figures

⏪

⏩

◀

▶

Back

Close

Full Screen / Esc

Printer-friendly Version

Interactive Discussion



friction velocity). Both meteorology and chemical concentration output fields are provided at 1 h time intervals.

3.2 The CHIMERE chemistry-transport model

CHIMERE is an off-line regional CTM forced by emissions (see Sect. 3.3), meteorological fields (see Sect. 3.1) and boundary conditions. The model version chimere2014 (Menut et al., 2013) is used here on the 50 km horizontal resolution grid described above. The vertical discretization consists in 18 uneven levels, from the surface up to 200 hPa.

The reduced chemical mechanism called MELCHIOR2 is used here and includes 44 species involved in almost 120 reactions. The list of species and reactions is provided in Menut et al. (2013). The aerosol module developed by Bessagnet et al. (2004) allows the simulation of primary particulate matter and secondary species: nitrates, sulphates, ammonium, primary organic matter (POM), secondary organic aerosol (SOA), elemental carbon (EC), marine aerosols and mineral dust. Their life cycle is represented with a complete scheme of nucleation, adsorption, desorption, coagulation, as well as wet and dry deposition and scavenging. The size distribution is simulated using a sectional representation, i.e using five bins from a diameter of 40 nm to 40 μ m.

Initial and boundary conditions are provided by 5 years monthly-averaged simulations by the global model LMDZ-INCA for aerosols and trace gases (Folberth et al., 2006), and GOCART for mineral dust (Ginoux et al., 2001).

The photolysis rates are calculated online using the Fast-JX module, version 7.0b (Wild et al., 2000; Bian et al., 2002) as described in Menut et al. (2013). The module computes the actinic fluxes by resolving the radiative transfer in the modelled atmospheric column. The treatment of optical properties is made by taking into account absorption by tropospheric and stratospheric ozone, Rayleigh scattering, absorption by aerosols, and Mie diffusion by aerosols and by liquid- and ice-water clouds. The total AOD is also obtained from these calculations at five different wavelengths: 200, 300, 400, 600 and 1000 nm (Mailler et al., 2015). As the calculation of the photolysis rates

Contributions to 2012 summertime aerosols in the Euro-Mediterranean region

G. Rea et al.

Title Page

Abstract

Introduction

Conclusions

References

Tables

Figures

◀

▶

◀

▶

Back

Close

Full Screen / Esc

Printer-friendly Version

Interactive Discussion



is performed at each physical time step taking into account the actualized concentrations of ozone and aerosols, this methodology allows retroaction of aerosol and ozone concentrations on photochemistry. In this study, the simulated AOD from CHIMERE at 500 and 550 nm are used and extracted by a linear interpolation from the output wavelengths.

3.3 Emissions

This section briefly describes the databases used for both primary particulate matter emissions and the emission of gaseous precursors.

Anthropogenic emissions are the only emissions that can be controlled; their inventories are updated constantly to take into account precise emissions in scenario studies. In this paper, the EDGAR-HTAP_V2 inventory for the reference year 2010 is used. It uses HTAP (Hemispheric Transport of Air Pollution) annual total masses which includes nationally reported emissions combined with regional scientific inventories, complemented with EDGARv4.3 data (http://edgar.jrc.ec.europa.eu/htap_v2). The inventory provides global annual emissions for CH₄, NMVOC, CO, SO₂, NO_x, NH₃, PM₁₀, PM_{2.5}, BC and OC, with a resolution of 0.1° × 0.1°. The annual emitted masses are disaggregated into model species and mapped onto the specified grid. Hourly emissions are estimated by applying seasonal, daily and weekly factors depending on the SNAP (Selected Nomenclature for Air Pollution) sectors. Anthropogenic emissions represent 90 to 100 % (among all other sources) of the regional emissions of NO_x, NH₃ and SO₂, which are important precursors of inorganic aerosol formation. For example, the total fluxes of NO_x in the region for the summer of 2012 are shown in Fig. 4. Anthropogenic emissions also amount to 53 % of primary organic matter emissions, 81 % of black carbon emissions, and 74 % of other primary particulate matter emissions.

Biogenic emissions fluxes are calculated using the global Model of Emissions of Gases and Aerosols from Nature (MEGAN; Guenther et al., 2006) and affect six CHIMERE species (isoprene, α -pinene, β -pinene, limonene, ocimene and NO). MEGAN is based on canopy-scale emission factors depending on the species. In their

Contributions to 2012 summertime aerosols in the Euro-Mediterranean region

G. Rea et al.

Title Page

Abstract

Introduction

Conclusions

References

Tables

Figures

◀

▶

◀

▶

Back

Close

Full Screen / Esc

Printer-friendly Version

Interactive Discussion



Contributions to 2012 summertime aerosols in the Euro-Mediterranean region

G. Rea et al.

Title Page

Abstract

Introduction

Conclusions

References

Tables

Figures



Back

Close

Full Screen / Esc

Printer-friendly Version

Interactive Discussion



analysis of isoprene emissions over Europe, Curci et al. (2010) compared CHIMERE simulation to satellite observations and found that MEGAN isoprene emissions might be 40 % higher over the Balkans, 20 % too high over Southern Germany, and 20 % too low over Iberian Peninsula, Greece and Italy. In Fig. 4, showing the calculated total biogenic fluxes of VOCs in Europe and the Mediterranean Basin during the summer of 2012, we can see that the majority of the emissions fluxes are located in the Balkans and Eastern Europe, and in general in the northern European part of the domain.

Mineral dust emissions use fluxes calculation with the Marticorena and Bergametti (1995) parametrisation for saltation and the optimized dust production model (Alfaro and Gomes, 2001; Menut et al., 2005) for sandblasting. The dust production model uses the model presented in Menut et al. (2013), which has been extended to be applicable to any region and not just North Africa (Briant et al., 2014). It uses new global soil and surface input datasets along with the global ASCAT/PARASOL aeolian roughness length dataset (Prigent et al., 2012). Parameterizations for humidity (Fecan et al., 1999) and seasonal vegetation variation were included. Since long-range transport from North Africa affects strongly the Mediterranean basin and Europe, the simulation domain was chosen in order to include western Africa and the Sahel, known to be active mineral dust sources (Israelevich et al., 2002; Prospero et al., 2002). On Fig. 4, representing the mineral dust emissions computed for the study, the majority of them are located in this region. Mineral dust particles are chemically inert in CHIMERE, but their size distribution is affected by wet and dry deposition. Dust emissions and deposition are strongly affected by meteorological fields, leading to large uncertainties (Menut et al., 2007, 2009).

Fire emissions are calculated using the APIFLAME v1.0 emissions model, described in Turquety et al. (2014), with a classical approach of multiplying the burned area by the fuel load consumed and the emission factors specific to the vegetation burned. The uncertainties concerning fire emissions are high, due to the accumulation of uncertainties on the emission factors, the area burned, the type of vegetation, etc. The uncertainty on the daily carbon emission is estimated at 100 % (Turquety et al., 2014), and using

The acronym associated with the sensitivity simulations undertaken for the study are ANTH, BIOG, FIRE, DUST, and SALT for the baseline simulation minus the simulation without anthropogenic, biogenic, fire, mineral dust and sea salt emissions, respectively.

Note that the sum of all individual sources may not amount to the reference concentrations of PM due to non-linearities in chemical processes. Differences have been evaluated for the summer of 2012 to be, on average over the domain, 1.3% of total PM_{2.5} for anthropogenic SOA, 2.3% for biogenic SOA and 4.8% for nitrates.

4 Evaluation of model results

This section presents the results of the reference simulation (all emissions included), evaluated against the observations presented in Sect. 2, to quantify the model performance for aerosol modelling.

4.1 Comparison with in situ PM surface concentrations

Surface PM simulation is evaluated using the correlation, the mean fractional error (MFE) and the mean fractional bias (MFB) between observations and collocated modelled surface concentrations. These statistical indicators are widely used in PM performance evaluation studies. Proposed by Boylan and Russell (2006) for PM, both the MFE and MFB must be lower than or equal to 50 and ± 30 % respectively to achieve the performance goals (level of accuracy considered to be close to the best a model can be expected to achieve), and must be lower than or equal to 75 and ± 60 % to meet the performance criteria (level of accuracy acceptable for standard modelling applications).

Tables 2 and 3 summarize the hourly and daily statistical results averaged over the regions NEU-We (393 stations for PM₁₀ and 133 for PM_{2.5}), NEU-Ce (266 and 10) and MED-We (92 and 13). Other regions do not contain enough AirBase stations to allow statistically significant comparison. For the time period and the entire domain of this study, the MFE and MFB on daily mean values are 42.9 and 21.6 % respectively for

Title Page

Abstract

Introduction

Conclusions

References

Tables

Figures

◀

▶

◀

▶

Back

Close

Full Screen / Esc

Printer-friendly Version

Interactive Discussion



Contributions to 2012 summertime aerosols in the Euro-Mediterranean region

G. Rea et al.

Title Page

Abstract

Introduction

Conclusions

References

Tables

Figures

◀

▶

◀

▶

Back

Close

Full Screen / Esc

Printer-friendly Version

Interactive Discussion

PM₁₀, and 44.3 and 31.8 % for PM_{2.5}. PM₁₀ daily mean values meet thus the performance goal. For hourly comparisons, performance goal is not met on average over the region (MFE = 52.8 % and MFB = 20.4 % for PM₁₀, MFE = 53.2 % and MFB = 32.4 % for PM_{2.5}), but the model performance criteria is met. Indeed, the performance criteria is met for more than 90 % of all the stations, and the performance goal is met for more than 40 % of them.

In the regional comparisons, highest differences are obtained in the MED-We region (82.6 % of the stations meet the performance criteria and only 16.3 % the performance goal for PM₁₀). Peak concentrations are often overestimated by the model for both PM₁₀ and PM_{2.5}, whereas levels are underestimated otherwise (MFB = −21.2 and −30.9 % respectively for PM₁₀ and PM_{2.5}). The MFB is relatively good for other regions (in general under 20 % except for NEU-We), indicating that PM concentrations do not have an excessive bias. The correlation coefficient is lower in the NEU-Ce region than in other regions (0.38 for PM₁₀ on 266 stations) for hourly comparisons (but not for daily averages with a correlation coefficient of 0.54). This suggests an influence of local sources for which the diurnal profiles used for the simulations may not be adapted to the region.

Figure 5 shows the temporal evolution of surface PM, averaged daily over the NEU-We, NEU-Ce and MED-We sub-regions. The levels of surface PM are consistent between observations and model, and the different peaks are well captured, especially in the northern part of the domain. In the Mediterranean Basin, levels are underestimated between 4 and 24 July where no peak is detected neither by observations nor by the model. Peaks of pollution during the end of July and August are slightly overestimated. For PM₁₀, in all three regions, a peak is overestimated by the model on 20 June by up to a factor of 4 (80 instead of 20 $\mu\text{g m}^{-3}$ in MED-We). High values (but lower) are observed for this date on some of the Mediterranean stations such as Miramas (Fig. 2) but not at other stations where the model overestimates strongly the peak value, particularly in the South of France. These peaks are attributed in Sect. 5.1 to a dust transport event. However, there is no associated overestimation of AOD values by the model compared

to the observations (MODIS or AERONET). This suggests that the overestimation in surface PM may be due to an overestimated transport at low altitudes, i.e. a wrong vertical distribution of the dust plumes. However, it may also be explained by an excess in total mass and a shift in the aerosol size distribution towards finer particles, as highlighted by Menut et al. (2015) through comparisons of CHIMERE simulations with AERONET retrievals of the size distribution. An excessive PM concentration would then result in a correct AOD due to the variation of the extinction efficiency with the size of the aerosol.

4.2 Comparison with Aerosol Optical Depth (AOD) measurements

To evaluate modeled AOD, we compare it to two dataset: MODIS satellite data and AERONET data at specific stations. For each statistic, we collocate in time and space the simulated AOD with the corresponding dataset. Figure 6 illustrates the time series of observed AOD and corresponding simulated values for each sub-region, and Table 4 the associated statistics. The modelled AOD is close to the observations in all regions except for NEU-We, with a correlation coefficient ranging from 0.54 (NEU-Ea) to 0.75 (MED-Ce) and a MFE of 36.50 % for comparisons to AERONET and 24.63 % for comparisons to MODIS. The simulated AOD is slightly underestimated in the eastern and southern parts of the domain, particularly compared to AERONET stations located in the eastern basin (MFB of -5.2% in MED-Ea). Compared to MODIS, the simulated AOD has a moderate underestimation (MFB of -39.8% in MED-Ea). This is also seen in the time series of Fig. 6. Highest values are seen in MED-We, and the model manages to reproduce these values at the right timing (highest correlation coefficient) even if it moderately underestimates them (MFB of -32.7% with respect to MODIS). Particularly, the peak at the beginning of July is underestimated by CHIMERE. The region with the lowest error and bias is MED-Ce, where the frequency and the intensity of peaks are lower.

5 Regional sensitivity to emission sources

In this section, the sensitivity of surface PM concentrations and total AOD to the different sources is analysed based on the series of sensitivity simulations described in Sect. 3.4.

5.1 Surface particulate matter

Average relative contributions during the summer of 2012 to surface PM_{2.5} and PM₁₀ over the domain are presented in Figs. 7 and 8. Table 5 summarizes the contributions in each sub-region of Table 1. As already highlighted in the general evaluation of the simulations, surface concentrations and total AOD are the largest over North Africa and the Mediterranean area, especially the Western Mediterranean area.

Table 5 shows that concentrations of PM₁₀ are about three times higher than those of PM_{2.5} (38.28 vs. 13 µg m⁻³ on average over the total period and domains). Surface PM₁₀ also presents a stronger spatial variability (concentrations of surface PM₁₀ ranges on average from 13.24 in NEU-Ea to 88.17 µg m⁻³ in MED-We, whereas concentrations of surface PM_{2.5} ranges from 9.46 in NEU-We to 15.66 µg m⁻³ in MED-Ce).

The two most important contributors in the domain are anthropogenic and mineral dust emissions, which account, on average, respectively for 52 and 17 % of surface PM_{2.5}, and 19 and 62 % of surface PM₁₀. Anthropogenic emissions clearly dominate both surface PM_{2.5} and PM₁₀ in the northern part of the domain (up to 90 %) but are also the main contribution to surface PM_{2.5} above the Mediterranean Basin (~ 50 %) and most particularly, as expected, around populated coastal areas.

Since the main dust emissions are located in North Africa, dust dominates the aerosol budget in this region. They also represent the main contribution to surface PM₁₀ concentrations in the western Mediterranean area (Spain, South of France and Italy). The average contribution of mineral dust in the MED-We region is estimated to 86 % for surface PM₁₀ and 44 % for PM_{2.5}. In this region, the mean concentration of surface PM₁₀ over the period is exceeding the European threshold of 50 µg m⁻³

($88.17 \mu\text{g m}^{-3}$). The contribution of mineral dust alone in this region is exceeding this threshold ($75.63 \mu\text{g m}^{-3}$). Long-range transport also results in significant contributions in Northern Europe (22 % of surface PM_{10} on average in region NEU-Ce).

Fire emissions are more sporadic and thus represent a lower contribution to the average surface concentrations. However, significant increase during the summer of 2012 is obtained in Spain and the Balkans, close to the main fire events (cf. Fig. 4). The maps show an impact reaching up to 20 % locally on average during the summer. The largest regional contribution is obtained for the MED-Ce region, with 12 % of $\text{PM}_{2.5}$ associated with fires.

As expected, sea salt emissions are the main contribution to PM above the Atlantic Ocean. However, their relative contribution above continents is low, except in the coastal areas and over North-Western Europe where it reaches 29 % of surface PM_{10} . Over coastal cities, the impact of sea salts at the surface can be as large as that of anthropogenic emissions. Biogenic emissions have an important contribution to PM in Central Europe, where they are mainly located (Fig. 4). They account for almost 20 % of surface $\text{PM}_{2.5}$ in the NEU-Ce region.

Figure 10 shows the temporal evolution of surface $\text{PM}_{2.5}$ and PM_{10} , and their associated source contributions, over the different sub-regions depicted in Table 1: NEU-We, NEU-Ce and NEU-Ea, MED-We, MED-Ce and MED-Ea. It shows that the daily variability above the chosen regions is large, especially for surface PM_{10} , with diverse contributions. The variability in the Northern part of the domain is mainly controlled by anthropogenic emissions. However, the NEU-We region is also frequently affected by mineral dust (20–21 June, 1 July, end of August) and by sea salts for surface PM_{10} concentrations. In the NEU-Ce and NEU-Ea regions, most of the large peaks in PM_{10} are attributed to mineral dust transport events.

Extreme concentrations are simulated in the Western and Central Mediterranean areas (MED-We and Ce), here again mainly due to large contributions from mineral dust emissions. These impact mainly surface PM_{10} , while $\text{PM}_{2.5}$ are often dominated by

Contributions to 2012 summertime aerosols in the Euro-Mediterranean region

G. Rea et al.

Title Page

Abstract

Introduction

Conclusions

References

Tables

Figures

◀

▶

◀

▶

Back

Close

Full Screen / Esc

Printer-friendly Version

Interactive Discussion

a more constant contribution from anthropogenic emissions. Fires are another significant contribution in these regions at the end of July and August for surface $PM_{2.5}$.

Comparisons to AirBase surface observations highlighted an overestimate of the largest PM_{10} peaks in the simulations in the NEU-We, NEU-Ce and MED-We regions (Fig. 10). This suggests that mineral dust transport at low altitudes is too large in the model.

5.2 Vertical distributions and AOD

Figure 11 presents the vertical distributions of PM in the simulations, averaged over each of the sub-regions. As already highlighted in the discussion above, surface concentrations are strongly affected by anthropogenic emissions, except in the western and central Mediterranean Basins, which are dominantly affected by mineral dust transport. In this area, the vertical contribution from dust range from the surface to about 4–5 km, which is an usual pattern compared to the climatology of Nabat et al. (2013). Dust affects mainly the free troposphere over the northern regions. Fires and biogenic emissions are also important contributions, particularly for $PM_{2.5}$. They often have maximum contributions in the lower troposphere. Sea salts contribute to PM_{10} in Western Europe and the Mediterranean region, as well as in the central Mediterranean region, but are confined to the lower-most troposphere.

Contributions to the total AOD, which includes the signature of aerosols over the full vertical column, follow the same general patterns as the contributions to surface PM_{10} discussed above (average relative contributions in Fig. 9 and Table 5). However, the contribution of sea salts remains very low (< 1 %), due to a low radiative impact but also to the fact that sea salts remain close to the surface and make thus a low contribution to the full vertical column load.

Temporal variability over the selected sub-regions shows that, similarly to what was obtained for surface PM, anthropogenic emissions control the variability in the NEU-We region, while mineral dust emissions are the main contribution in the MED-We region. The fire episodes of the end of August also contribute significantly to the total AOD in

Title Page

Abstract

Introduction

Conclusions

References

Tables

Figures



Back

Close

Full Screen / Esc

Printer-friendly Version

Interactive Discussion



the NEU-Ea and MED-Ce regions. Compared to the total column (vertically integrated) concentrations of PM, contributions from fine particles to AOD are larger. This is due to the fact that fine particles from anthropogenic or fire emissions, even concentrated in the first layers, are more active optically than larger mineral dust particles at the considered wavelength (500 nm), and hence contribute more significantly to the calculated AOD.

6 Contributions to air quality threshold exceedances

The European Union has developed legislations to establish health based standards for a number of atmospheric pollutants. For PM₁₀, the limit is a daily mean of 50 µg m⁻³ and an annual mean of 40 µg m⁻³. In this section, the exceedances of the daily mean limit for PM₁₀ concentrations are analysed. The number of stations in daily exceedances are calculated for both AirBase observations and collocated CHIMERE simulations. The simulations were undertaken at a regional scale, so that only exceedances at rural and background sites are considered.

In total, 96.2 % of the daily means are under the threshold of 50 µg m⁻³ in both observations and co-located simulation. The analysis will focus on the 3.8 % other cases. Figure 12 presents the number of stations where the daily mean concentration of PM₁₀ is above 50 µg m⁻³, in the observations or the model simulations within each sub-region (only the sub-regions where there are AirBase stations to compare with).

It clearly shows that the model detects more exceedances than the observations (in total 1965 vs. 624 in the observations, positive bias from 54.5, 82.2 and 72.2 % for respectively MED-We, NEU-We and NEU-Ce), and sometimes not at the same time (correlation coefficient of respectively 0.6, 0.48 and 0.4). 43.6 % of the 624 observed exceedances are correctly captured by the model, the majority of them located in MED-We. More particularly, the event of 27–28 June is well simulated (cf. Fig. 2) and is correctly detected in terms of number of stations in daily exceedances (29 exceedances

Contributions to 2012 summertime aerosols in the Euro-Mediterranean region

G. Rea et al.

Title Page

Abstract

Introduction

Conclusions

References

Tables

Figures

◀

▶

◀

▶

Back

Close

Full Screen / Esc

Printer-friendly Version

Interactive Discussion



for observations, 35 for the model, among the 92 stations). This is also the case for the two peaks in August (around 20–30 exceedances).

Figure 13 shows the contribution of each source when the concentration exceeds the threshold for both model and observations. For these peaks, the contribution of mineral dust is predominant, mixed with anthropogenic pollution and fires from 28 June to 3 July (fires alone contribute to 3 exceedances at that time), as well as biogenic emissions from 18 to 23 August.

The peak of the 20–21 June is present in the model simulations at almost every AirBase stations, but only at some stations in the observations (see Sect. 4.1). The number of simulated exceedances is thus a lot larger than in the AirBase dataset. This peak is attributed to a mineral dust event that is overestimated by the model in most of the stations, with a high contribution in MED-We, and a lower contribution in other regions (mixed with anthropogenic and biogenic contributions).

Exceedances are also detected at the end of July, between 27 and 31, in the three sub-regions. The model here again overestimates the number of stations in daily exceedances (37 vs. 6 for observations in MED-We, 82 vs. 14 for NEU-We). The sensitivity simulations indicate that the concentration of PM was high due to contributions from all the different sources: mineral dust mainly, anthropogenic, and fires (stronger in MED-We and NEU-Ce) associated to biogenic in NEU-We and NEU-Ce.

In MED-We, 240 exceedances are seen by both the model and the observations. Without the anthropogenic sources, there are still 222 exceedances, so that 92.5% of them are due to natural sources according to CHIMERE. In NEU-We, on the 17 exceedances detected by both the model and the observations, 35.3% are due to natural sources. Finally in NEU-Ce, 75% of the 13 coherent exceedances are due to natural sources.

Using a linear regression on modelled vs. observed PM_{10} concentrations when the contribution of mineral dust is more than 60%, the model values corresponding to the $50 \mu g m^{-3}$ limit in the observations are found to be 75, 58 and $62 \mu g m^{-3}$ for MED-We, NEU-We and NEU-Ce, respectively. Setting higher daily limits values for the model

Contributions to 2012 summertime aerosols in the Euro-Mediterranean region

G. Rea et al.

Title Page

Abstract

Introduction

Conclusions

References

Tables

Figures

◀

▶

◀

▶

Back

Close

Full Screen / Esc

Printer-friendly Version

Interactive Discussion



(in the detection of an exceedance) only for dust events could result in better agreement between modelled and observed number of stations in daily exceedance. The corresponding comparisons are shown in Fig. 12 (dashed red line). This method allows a slight reduction of the biases (from 54.5 to 34.5 % for MED-We, from 82.2 to 74.9 % for NEU-We, and from 72.2 to 48.6 % for NEU-Ce). However, large discrepancies remain on some events, showing that this does not resolve the modelled excessive spatial spread and intensity of some mineral dust events.

This analysis shows that air quality levels remain difficult to diagnose for this regional simulation. Exceedances due to mineral dust are well captured by the model in the sub-region closest to the mineral dust outflow (MED-We), except for the event of 20–21 July. In other sub-regions, CHIMERE overestimates pollution levels attributed to mineral dust above many stations, indicating that plumes are either simulated at too low altitudes, either too spread over the region. Fires also represent a large source of uncertainty for the peak around the 25 July in MED-We. In other regions, the mix between mineral dust, anthropogenic and biogenic sources leads to exceedances in the model not systematically seen at the stations and vice versa. Even if natural sources as mineral dust events are particularly difficult to estimate, their contribution to the exceedances of the limitation appears preponderant during the summer of 2012 (from 35 % in NEU-Ce to 92.5 % in MED-We).

7 Conclusions

A sensitivity analysis was undertaken over Europe and the Mediterranean region to estimate the contribution of anthropogenic, mineral dust, fire, biogenic and sea salt emissions on surface PM_{10} , surface $PM_{2.5}$ and total AOD during the summer of 2012. Therefore, simulations were performed using the CHIMERE regional CTM, including all sources (reference simulation) and removing one of these source at a time (sensitivity study).

Contributions to 2012 summertime aerosols in the Euro-Mediterranean region

G. Rea et al.

Title Page

Abstract

Introduction

Conclusions

References

Tables

Figures

◀

▶

◀

▶

Back

Close

Full Screen / Esc

Printer-friendly Version

Interactive Discussion



**Contributions to 2012
summertime aerosols
in the
Euro-Mediterranean
region**

G. Rea et al.

[Title Page](#)[Abstract](#)[Introduction](#)[Conclusions](#)[References](#)[Tables](#)[Figures](#)[◀](#)[▶](#)[◀](#)[▶](#)[Back](#)[Close](#)[Full Screen / Esc](#)[Printer-friendly Version](#)[Interactive Discussion](#)

The reference simulation has been evaluated against observations of surface PM from the AirBase network, and of AOD from the AERONET network and the MODIS space-based instrument. Although the density of the AirBase network is relatively high in parts of Europe, there is a lack of observations around the Mediterranean Basin, which thus cannot be evaluated in terms of surface PM concentrations.

For the northern part of the domain and the western Mediterranean Basin, the comparison between CHIMERE simulations and the AirBase observations ($PM_{2.5}$ and PM_{10}) has shown the ability of the model to simulate PM levels (the performance criteria are met for hourly values for more than 90 % of the stations, i.e. both MFE and MFB are lower than or equal to 75 and ± 60 % respectively). However, the associated variability is not well established with the correlation ranging from 0.38 to 0.49 depending on the region. All the main peaks are though reproduced by the model. The MFB is under 20 % over the area, with some overestimations of peaks in the south west of the domain. The correlation is lower in the center north, where local sources strongly influence observations. This influence cannot be captured at the resolution used for the simulation (50 km). On the contrary, some peak values are overestimated in the northern part of the domain by up to a factor of 4.

The comparison between simulated AOD and observations from AERONET and MODIS also shows good results with a correlation ranging from 0.35 to 0.75, and a reasonable MFE (36.2 % with respect to AERONET and 24.6 % with respect to MODIS). An underestimation is seen in the eastern and southern part of the domain (MFB up to about -39.8 %).

Results of sensitivity simulations show that the Euro-Mediterranean domain is strongly influenced by mineral dust transport and anthropogenic emissions (62 and 19 % respectively for surface PM_{10} and 17 and 52 % for surface $PM_{2.5}$). For mineral dust, the contribution is particularly important in the western Mediterranean Basin (86 % for surface PM_{10} and 44 % for $PM_{2.5}$) where the concentrations are the highest. In this region, all the extreme peaks are attributed to this source. In the northern part of the domain, mineral dust affects mainly the free troposphere. At the surface, anthro-

References

- Alfaro, S. C. and Gomes, L.: Modeling mineral aerosol production by wind erosion: emission intensities and aerosol size distributions in source areas, *J. Geophys. Res.-Atmos.*, 106, 18075–18084, doi:10.1029/2000JD900339, 2001. 8204
- 5 Anttila, P., Stefanovska, A., Nestorovska-Krsteska, A., Grozdanovski, L., Atanasov, I., Golubov, N., Ristevski, P., Toceva, M., Lappi, S., and Walden, J.: Characterisation of extreme air pollution episodes in an urban valley in the Balkan Peninsula, *Air Quality, Atmosphere & Health*, 1–13, doi:10.1007/s11869-015-0326-7, 2015. 8195
- Barnaba, F., Angelini, F., Curci, G., and Gobbi, G. P.: An important fingerprint of wildfires on the European aerosol load, *Atmos. Chem. Phys.*, 11, 10487–10501, doi:10.5194/acp-11-10487-2011, 2011. 8195
- 10 Bessagnet, B., Hodzic, A., Vautard, R., Beekmann, M., Cheinet, S., Honoré, C., Liousse, C., and Rouil, L.: Aerosol modeling with CHIMERE: preliminary evaluation at the continental scale, *Atmos. Environ.*, 38, 2803–2817, doi:10.1016/j.atmosenv.2004.02.034, 2004. 8202
- 15 Bian, H. and Prather, M.: Fast-J2: accurate simulation of stratospheric photolysis in global chemical models, *J. Atmos. Chem.*, 41, 281–296, 2002. 8202
- Boldo, E., Medina, S., Le Tertre, A., Hurley, F., Mücke, H.-G., Ballester, F., and Aguilera, I.: Apehis: Health impact assessment of long-term exposure to PM_{2.5} in 23 European cities, *Eur. J. Epidemiol.*, 21, 449–458, 2006. 8193
- 20 Boselli, A., Caggiano, R., Cornacchia, C., Madonna, F., Mona, L., Macchiato, M., Pappalardo, G., and Trippetta, S.: Multi year sun-photometer measurements for aerosol characterization in a Central Mediterranean site, *Atmos. Res.*, 104, 98–110, 2012. 8194
- Boylan, J. W. and Russell, A. G.: PM and light extinction model performance metrics, goals, and criteria for three-dimensional air quality models, *Atmos. Environ.*, 40, 4946–4959, 2006. 8206
- 25 Briant, R., Menut, L., Siour, G., and Prigent, C.: Homogenized modeling of mineral dust emissions over Europe and Africa using the CHIMERE model, *Geosci. Model Dev. Discuss.*, 7, 3441–3480, doi:10.5194/gmdd-7-3441-2014, 2014. 8204
- Carlsaw, K. S., Boucher, O., Spracklen, D. V., Mann, G. W., Rae, J. G. L., Woodward, S., and Kulmala, M.: A review of natural aerosol interactions and feedbacks within the Earth system, *Atmos. Chem. Phys.*, 10, 1701–1737, doi:10.5194/acp-10-1701-2010, 2010. 8193
- 30

**Contributions to 2012
summertime aerosols
in the
Euro-Mediterranean
region**

G. Rea et al.

[Title Page](#)[Abstract](#)[Introduction](#)[Conclusions](#)[References](#)[Tables](#)[Figures](#)[◀](#)[▶](#)[◀](#)[▶](#)[Back](#)[Close](#)[Full Screen / Esc](#)[Printer-friendly Version](#)[Interactive Discussion](#)

Curci, G., Palmer, P. I., Kurosu, T. P., Chance, K., and Visconti, G.: Estimating European volatile organic compound emissions using satellite observations of formaldehyde from the Ozone Monitoring Instrument, *Atmos. Chem. Phys.*, 10, 11501–11517, doi:10.5194/acp-10-11501-2010, 2010. 8204

5 DalliOsto, M., Harrison, R. M., Highwood, E. J., ODowd, C., Ceburnis, D., Querol, X., and Achterberg, E. P.: Variation of the mixing state of Saharan dust particles with atmospheric transport, *Atmos. Environ.*, 44, 3135–3146, 2010. 8194

Daskalakis, N., Myriokefalitakis, S., and Kanakidou, M.: Sensitivity of tropospheric loads and lifetimes of short lived pollutants to fire emissions, *Atmos. Chem. Phys. Discuss.*, 14, 22639–22676, doi:10.5194/acpd-14-22639-2014, 2014. 8205

10 Dubovik, O., Smirnov, A., Holben, B., King, M., Kaufman, Y., Eck, T., and Slutsker, I.: Accuracy assessments of aerosol optical properties retrieved from Aerosol Robotic Network (AERONET) sun and sky radiance measurements, *J. Geophys. Res.-Atmos.*, 105, 9791–9806, 2000. 8199

15 Dudhia, J.: Numerical study of convection observed during the winter monsoon experiment using a mesoscale two-dimensional model, *J. Atmos. Sci.*, 46, 3077–3107, 1989. 8201

Fecan, F., Marticorena, B., and Bergametti, G.: Parameterization of the increase of aeolian erosion threshold wind friction velocity due to soil moisture for arid and semi-arid areas, *Ann. Geophys.-Italy*, 17, 149–157, 1999. 8204

20 Folberth, G. A., Hauglustaine, D. A., Lathière, J., and Brocheton, F.: Interactive chemistry in the Laboratoire de Météorologie Dynamique general circulation model: model description and impact analysis of biogenic hydrocarbons on tropospheric chemistry, *Atmos. Chem. Phys.*, 6, 2273–2319, doi:10.5194/acp-6-2273-2006, 2006. 8202

25 Gerasopoulos, E., Kouvarakis, G., Babasakalis, P., Vrekoussis, M., Putaud, J.-P., and Mihalopoulos, N.: Origin and variability of particulate matter (PM₁₀) mass concentrations over the Eastern Mediterranean, *Atmos. Environ.*, 40, 4679–4690, 2006. 8194

Gerasopoulos, E., Amiridis, V., Kazadzis, S., Kokkalis, P., Eleftheratos, K., Andreae, M. O., Andreae, T. W., El-Askary, H., and Zerefos, C. S.: Three-year ground based measurements of aerosol optical depth over the Eastern Mediterranean: the urban environment of Athens, *Atmos. Chem. Phys.*, 11, 2145–2159, doi:10.5194/acp-11-2145-2011, 2011. 8194

30 Ginoux, P., Chin, M., Tegen, I., Prospero, J. M., Holben, B., Dubovik, O., and Lin, S. J.: Sources and distributions of dust aerosols simulated with the GOCART model, *J. Geophys. Res.*, 106, 20255–20273, 2001. 8202

**Contributions to 2012
summertime aerosols
in the
Euro-Mediterranean
region**

G. Rea et al.

[Title Page](#)[Abstract](#)[Introduction](#)[Conclusions](#)[References](#)[Tables](#)[Figures](#)[◀](#)[▶](#)[◀](#)[▶](#)[Back](#)[Close](#)[Full Screen / Esc](#)[Printer-friendly Version](#)[Interactive Discussion](#)

- Gobbi, G., Barnaba, F., and Ammannat, L.: Estimating the impact of Saharan dust on the year 2001 PM₁₀ record of Rome, Italy, *Atmos. Environ.*, 41, 261–275, 2007. 8194
- Gómez-Amo, J. L., Estellés, V., Segura, S., Marcos, C., Esteve, A. R., Pedrós, R., Utrillas, M. P., and Martínez-Lozano, J. A.: Analysis of a strong wildfire event over Valencia (Spain) during Summer 2012 – Part 1: Aerosol microphysics and optical properties, *Atmos. Chem. Phys. Discuss.*, 13, 22639–22685, doi:10.5194/acpd-13-22639-2013, 2013. 8195
- Guenther, A., Karl, T., Harley, P., Wiedinmyer, C., Palmer, P. I., and Geron, C.: Estimates of global terrestrial isoprene emissions using MEGAN (Model of Emissions of Gases and Aerosols from Nature), *Atmos. Chem. Phys.*, 6, 3181–3210, doi:10.5194/acp-6-3181-2006, 2006. 8203
- Hansen, J., Sato, M., and Ruedy, R.: Radiative forcing and climate response, *J. Geophys. Res.-Atmos.*, 102, 6831–6864, doi:10.1029/96JD03436, 1997. 8193
- Hodzic, A., Madronich, S., Bohn, B., Massie, S., Menut, L., and Wiedinmyer, C.: Wildfire particulate matter in Europe during summer 2003: meso-scale modeling of smoke emissions, transport and radiative effects, *Atmos. Chem. Phys.*, 7, 4043–4064, doi:10.5194/acp-7-4043-2007, 2007. 8195
- Holben, B., Eck, T., Slutsker, I., Tanré, D., Buis, J., Setzer, A., Vermote, E., Reagan, J., Kaufman, Y., Nakajima, T., Lavenu, F., Jankowiak, I., and Smirnov, A.: AERONET – a federated instrument network and data archive for aerosol characterization, *Remote Sens. Environ.*, 66, 1–16, 1998. 8199
- Hong, S.-Y. and Lim, J.-O. J.: The WRF single-moment 6-class microphysics scheme (WSM6), *J. Korean Meteor. Soc.*, 42, 129–151, 2006. 8201
- Iacono, M. J., Delamere, J. S., Mlawer, E. J., Shephard, M. W., Clough, S. A., and Collins, W. D.: Radiative forcing by long-lived greenhouse gases: calculations with the AER radiative transfer models, *J. Geophys. Res.-Atmos.*, 113, D13103, doi:10.1029/2008JD009944, 2008. 8201
- Israelevich, P., Ganor, E., Alpert, P., Kishcha, P., and Stupp, A.: Predominant transport paths of Saharan dust over the Mediterranean Sea to Europe, *J. Geophys. Res.-Atmos.*, 117, D02205, doi:10.1029/2011JD016482, 2012. 8194
- Israelevich, P. L., Levin, Z., Joseph, J. H., and Ganor, E.: Desert aerosol transport in the Mediterranean region as inferred from the TOMS aerosol index, *J. Geophys. Res.-Atmos.*, 107, AAC13-1–AAC13-13, doi:10.1029/2001JD002011, 2002. 8204
- Janjic, Z.: The Surface Layer Parameterization in the NCEP Eta Model, *World Meteorological Organization-Publications-WMO TD*, 4–16, 1996. 8201

Contributions to 2012 summertime aerosols in the Euro-Mediterranean region

G. Rea et al.

Title Page

Abstract

Introduction

Conclusions

References

Tables

Figures

◀

▶

◀

▶

Back

Close

Full Screen / Esc

Printer-friendly Version

Interactive Discussion

- Kain, J. S.: Convective parameterization for mesoscale models: the Kain–Fritsch scheme, the representation of cumulus convection in numerical models, *Meteor. Mon.*, 46, 165–170, 1993. 8201
- 5 Kalnay, E., Kanamitsu, M., Kistler, R., Collins, W., Deaven, D., Gandin, L., Iredell, M., Saha, S., White, G., Woollen, J., Zhu, Y., Chelliah, M., Ebisuzaki, W., Higgins, W., Janowiak, J., Mo, K., Ropelewski, C., Wang, J., Leetmaa, A., Reynolds, R., Jenne, R., and Joseph, D.: The NCEP/NCAR 40-year reanalysis project, *B. Am. Meteorol. Soc.*, 77, 437–471, 1996. 8201
- 10 Kaskaoutis, D., Kambezidis, H., Nastos, P., and Kosmopoulos, P.: Study on an intense dust storm over Greece, *Atmos. Environ.*, 42, 6884–6896, 2008. 8194
- Katsouyanni, K., Touloumi, G., Spix, C., Schwartz, J., Balducci, F., Medina, S., Rossi, G., Wojtyniak, B., Sunyer, J., Bacharova, L., Schouten, J. P., Ponka, A., and Anderson, H. R.: Short term effects of ambient sulphur dioxide and particulate matter on mortality in 12 European cities: results from time series data from the APHEA project, *BMJ*, 314, 1658, doi:10.1136/bmj.314.7095.1658, 1997. 8193
- 15 Koçak, M., Mihalopoulos, N., and Kubilay, N.: Contributions of natural sources to high PM₁₀ and PM_{2.5} events in the eastern Mediterranean, *Atmos. Environ.*, 41, 3806–3818, 2007. 8194
- Lionello, P., Malanotte-Rizzoli, P., Boscolo, R., Alpert, P., Artale, V., Li, L., Luterbacher, J., May, W., Trigo, R., Tsimplis, M., Ulbrich, U., and Xoplaki, E.: The Mediterranean climate: an overview of the main characteristics and issues, *Developments in Earth and Environmental Sciences*, 4, 1–26, 2006. 8193
- 20 Mailler, S., Menut, L., Di Sarra, A. G., Becagli, S., Di Iorio, T., Formenti, P., Bessagnet, B., Briant, R., Gmez-Amo, J. L., Mallet, M., Rea, G., Siour, G., Sferlazzo, D. M., Traversi, R., Udisti, R., and Turquety, S.: On the radiative impact of aerosols on photolysis rates: comparison of simulations and observations in the Lampedusa island during the CharMEx/ADRI-MED campaign, *Atmos. Chem. Phys. Discuss.*, 15, 7585–7643, doi:10.5194/acpd-15-7585-2015, 2015. 8195, 8202
- 25 Marticorena, B. and Bergametti, G.: Modeling the atmospheric dust cycle: 1. Design of a soil-derived dust emission scheme, *J. Geophys. Res.-Atmos.*, 100, 16415–16430, doi:10.1029/95JD00690, 1995. 8204
- 30 Menut, L., Schmechtig, C., and Marticorena, B.: Sensitivity of the sandblasting fluxes calculations to the soil size distribution accuracy, *J. Atmos. Ocean. Tech.*, 22, 1875–1884, doi:10.1175/JTECH1825.1, 2005. 8204

**Contributions to 2012
summertime aerosols
in the
Euro-Mediterranean
region**

G. Rea et al.

Title Page

Abstract

Introduction

Conclusions

References

Tables

Figures

◀

▶

◀

▶

Back

Close

Full Screen / Esc

Printer-friendly Version

Interactive Discussion

- Menut, L., Foret, G., and Bergametti, G.: Sensitivity of mineral dust concentrations to the model size distribution accuracy, *J. Geophys. Res.-Atmos.*, 112, D10210, doi:10.1029/2006JD007766, 2007. 8204
- Menut, L., Chiapello, I., and Moulin, C.: Previsibility of mineral dust concentrations: the CHIMERE-DUST forecast during the first AMMA experiment dry season, *J. Geophys. Res.*, 114, D07202, doi:10.1029/2008JD010523, 2009. 8204
- Menut, L., Bessagnet, B., Khvorostyanov, D., Beekmann, M., Blond, N., Colette, A., Coll, I., Curci, G., Foret, G., Hodzic, A., Mailler, S., Meleux, F., Monge, J.-L., Pison, I., Siour, G., Turquety, S., Valari, M., Vautard, R., and Vivanco, M. G.: CHIMERE 2013: a model for regional atmospheric composition modelling, *Geosci. Model Dev.*, 6, 981–1028, doi:10.5194/gmd-6-981-2013, 2013. 8196, 8202, 8204
- Menut, L., Mailler, S., Siour, G., Bessagnet, B., Turquety, S., Rea, G., Briant, R., Mallet, M., Sciare, J., and P, F.: Ozone and aerosols tropospheric concentrations variability analyzed using the ADRIMED measurements and the WRF-CHIMERE models, *Atmos. Chem. Phys. Discuss.*, 15, 3063–3125, doi:10.5194/acpd-15-3063-2015, 2015. 8208
- Millán, M. M., José Sanz, M., Salvador, R., and Mantilla, E.: Atmospheric dynamics and ozone cycles related to nitrogen deposition in the western Mediterranean, *Environ. Pollut.*, 118, 167–186, 2002. 8193
- Monahan, E. C.: The ocean as a source of atmospheric particles, in: *The Role of Air–Sea Exchange in Geochemical Cycling*, Kluwer Academic Publishers, Dordrecht, Holland, 129–163, 1986. 8205
- Monks, P., Granier, C., Fuzzi, S., Stohl, A., Williams, M., Akimoto, H., Amann, M., Baklanov, A., Baltensperger, U., Bey, I., Blake, N., Blake, R., Carslaw, K., Cooper, O., Dentener, F., Fowler, D., Fragkou, E., Frost, G., Generoso, S., Ginoux, P., Grewe, V., Guenther, A., Hansson, H., Henne, S., Hjorth, J., Hofzumahaus, A., Huntrieser, H., Isaksen, I., Jenkin, M., Kaiser, J., Kanakidou, M., Klimont, Z., Kulmala, M., Laj, P., Lawrence, M., Lee, J., Liousse, C., Maione, M., McFiggans, G., Metzger, A., Mieville, A., Moussiopoulos, N., Orlando, J., O’Dowd, C., Palmer, P., Parrish, D., Petzold, A., Platt, U., Pschl, U., Prvt, A., Reeves, C., Reimann, S., Rudich, Y., Sellegri, K., Steinbrecher, R., Simpson, D., ten Brink, H., Theloke, J., van der Werf, G., Vautard, R., Vestreng, V., Vlachokostas, C., and von Glasow, R.: Atmospheric composition change – global and regional air quality, *Atmos. Environ.*, 43, 5268–5350, doi:10.1016/j.atmosenv.2009.08.021, 2009. 8193, 8194

**Contributions to 2012
summertime aerosols
in the
Euro-Mediterranean
region**

G. Rea et al.

[Title Page](#)[Abstract](#)[Introduction](#)[Conclusions](#)[References](#)[Tables](#)[Figures](#)[◀](#)[▶](#)[◀](#)[▶](#)[Back](#)[Close](#)[Full Screen / Esc](#)[Printer-friendly Version](#)[Interactive Discussion](#)

Brink, H., Tursic, J., Viana, M., Wiedensohler, A., and Raes, F.: A European aerosol phenomenology – 3: Physical and chemical characteristics of particulate matter from 60 rural, urban, and kerbside sites across Europe, *Atmos. Environ.*, 44, 1308–1320, 2010. 8193

Remer, L. A., Kaufman, Y. J., Tanré, D., Mattoo, S., Chu, D. A., Martins, J. V., Li, R.-R., Ichoku, C., Levy, R. C., Kleidman, R. G., Eck, T. F., Vermote, E., and Holben, B. N.: The MODIS aerosol algorithm, products and validation, special section, *J. Atmos. Sci.*, 62, 947–973, 2005. 8199

Remer, L. A., Tanre, D., Kaufman, Y. J., Levy, R., and Mattoo, S.: Algorithm For Remote Sensing of Tropospheric Aerosol From MODIS: Collection 005, National Aeronautics and Space Administration, 2006. 8199

Ripoll, A., Minguillón, M. C., Pey, J., Pérez, N., Querol, X., and Alastuey, A.: Joint analysis of continental and regional background environments in the western Mediterranean: PM₁ and PM₁₀ concentrations and composition, *Atmos. Chem. Phys.*, 15, 1129–1145, doi:10.5194/acp-15-1129-2015, 2015. 8194

Rodriguez, S., Querol, X., Alastuey, A., and de la Rosa, J.: Atmospheric particulate matter and air quality in the Mediterranean: a review, *Environ. Chem. Lett.*, 5, 1–7, doi:10.1007/s10311-006-0071-0, 2007. 8194

Roustan, Y., Sartelet, K., Tombette, M., Debry, É., and Sportisse, B.: Simulation of aerosols and gas-phase species over Europe with the POLYPHEMUS system, Part II: Model sensitivity analysis for 2001, *Atmos. Environ.*, 44, 4219–4229, 2010. 8196

Salvador, P., Alonso-Pérez, S., Pey, J., Artíñano, B., de Bustos, J. J., Alastuey, A., and Querol, X.: African dust outbreaks over the western Mediterranean Basin: 11-year characterization of atmospheric circulation patterns and dust source areas, *Atmos. Chem. Phys.*, 14, 6759–6775, doi:10.5194/acp-14-6759-2014, 2014. 8194

Sartelet, K. N., Couvidat, F., Seigneur, C., and Roustan, Y.: Impact of biogenic emissions on air quality over Europe and North America, *Atmos. Environ.*, 53, 131–141, 2012. 8194, 8196

Sayer, A. M., Hsu, N. C., Bettenhausen, C., and Jeong, M.-J.: Validation and uncertainty estimates for MODIS collection 6 “Deep Blue” aerosol data, *J. Geophys. Res.-Atmos.*, 118, 7864–7872, 2013. 8199

Skamarock, W., Klemp, J., Dudhia, J., Gill, D., Barker, D., Duda, M., Huang, X., Wang, W., and Powers, J.: A Description of the Advanced Research WRF Version 3., NCAR Technical Note, 123 pp., 2008. 8201

**Contributions to 2012
summertime aerosols
in the
Euro-Mediterranean
region**

G. Rea et al.

[Title Page](#)[Abstract](#)[Introduction](#)[Conclusions](#)[References](#)[Tables](#)[Figures](#)[◀](#)[▶](#)[◀](#)[▶](#)[Back](#)[Close](#)[Full Screen / Esc](#)[Printer-friendly Version](#)[Interactive Discussion](#)

- Solazzo, E., Bianconi, R., Pirovano, G., Matthias, V., Vautard, R., Moran, M. D., Appel, K. W., Bessagnet, B., Brandt, J., Christensen, J. H., Chemel, C., Coll, I., Ferreira, J., Forkel, R., Francis, X. V., Grell, G., Grossi, P., Hansen, A. B., Miranda, A. I., Nopmongcol, U., Prank, M., Sartelet, K. N., Schaap, M., Silver, J. D., Sokhi, R. S., Vira, J., Werhahn, J., Wolke, R., Yarwood, G., Zhang, J., Rao, S. T., and Galmarini, S.: Operational model evaluation for particulate matter in Europe and North America in the context of AQMEII, *Atmos. Environ.*, 53, 75–92, doi:10.1016/j.atmosenv.2012.02.045, 2012. 8196
- 5 Stocker, T., Qin, D., Plattner, G., Tignor, M., Allen, S., Boschung, J., Nauels, A., Xia, Y., Bex, V., and Midgley, P.: Climate Change 2013: The Physical Science Basis, Contribution of Working Group I to the Fifth Assessment Report of the Intergovernmental Panel on Climate Change, 2013. 8193
- 10 Textor, C., Schulz, M., Guibert, S., Kinne, S., Balkanski, Y., Bauer, S., Berntsen, T., Berglen, T., Boucher, O., Chin, M., Dentener, F., Diehl, T., Easter, R., Feichter, H., Fillmore, D., Ghan, S., Ginoux, P., Gong, S., Grini, A., Hendricks, J., Horowitz, L., Huang, P., Isaksen, I., Iversen, I., Kloster, S., Koch, D., Kirkevåg, A., Kristjansson, J. E., Krol, M., Lauer, A., Lamarque, J. F., Liu, X., Montanaro, V., Myhre, G., Penner, J., Pitari, G., Reddy, S., Seland, Ø., Stier, P., Takemura, T., and Tie, X.: Analysis and quantification of the diversities of aerosol life cycles within AeroCom, *Atmos. Chem. Phys.*, 6, 1777–1813, doi:10.5194/acp-6-1777-2006, 2006. 8193
- 15 20 Turquety, S., Menut, L., Bessagnet, B., Anav, A., Viovy, N., Maignan, F., and Wooster, M.: API-FLAME v1.0: high-resolution fire emission model and application to the Euro-Mediterranean region, *Geosci. Model Dev.*, 7, 587–612, doi:10.5194/gmd-7-587-2014, 2014. 8195, 8204
- Wild, O., Zhu, X., and Prather, J.: Fast-J: accurate simulation of the in- and below-cloud photolysis in tropospheric chemical models, *J. Atmos. Chem.*, 37, 245–282, 2000. 8202
- 25 Yu, H., Kaufman, Y. J., Chin, M., Feingold, G., Remer, L. A., Anderson, T. L., Balkanski, Y., Bellouin, N., Boucher, O., Christopher, S., DeCola, P., Kahn, R., Koch, D., Loeb, N., Reddy, M. S., Schulz, M., Takemura, T., and Zhou, M.: A review of measurement-based assessments of the aerosol direct radiative effect and forcing, *Atmos. Chem. Phys.*, 6, 613–666, doi:10.5194/acp-6-613-2006, 2006. 8193

Contributions to 2012 summertime aerosols in the Euro-Mediterranean region

G. Rea et al.

Table 2. Hourly performance statistics for the simulation of PM with CHIMERE (Mod.) compared to AirBase measurements (Obs.) during the summer of 2012.

Variable	Region	Number of stations	Mean		<i>R</i>	RMSE	MFB	MFB	MFE
			Obs.	Mod.					
PM ₁₀	NEU-We	393	16.70	17.07	0.40	13.26	−1.83 %	19.83 %	50.28 %
	NEU-Ce	266	17.22	16.13	0.38	13.75	−5.69 %	17.45 %	52.99 %
	MED-We	92	25.97	25.20	0.42	27.86	−21.16 %	30.78 %	63.20 %
	ALL	760	18.08	17.93	0.39	15.38	−5.34 %	20.42 %	52.80 %
PM _{2.5}	NEU-We	133	9.76	11.73	0.49	8.20	18.36 %	33.56 %	54.33 %
	NEU-Ce	10	10.91	11.74	0.41	6.61	11.03 %	22.68 %	45.35 %
	MED-We	13	14.46	11.24	0.37	9.62	−30.86 %	33.59 %	56.06 %
	ALL	161	10.44	11.88	0.48	8.24	13.36 %	32.35 %	53.18 %

[Title Page](#)
[Abstract](#)
[Introduction](#)
[Conclusions](#)
[References](#)
[Tables](#)
[Figures](#)
[Back](#)
[Close](#)
[Full Screen / Esc](#)
[Printer-friendly Version](#)
[Interactive Discussion](#)

Contributions to 2012 summertime aerosols in the Euro-Mediterranean region

G. Rea et al.

Table 3. Daily performance statistics for the simulation of PM with CHIMERE (Mod.) compared to AirBase measurements (Obs.) during the summer of 2012.

Variable	Region	Number of stations	Mean		<i>R</i>	RMSE	MFB	MFB	MFE
			Obs.	Mod.					
PM ₁₀	NEU-We	393	16.63	17.04	0.53	10.45	−3.38 %	19.67 %	40.30 %
	NEU-Ce	266	17.28	16.16	0.54	10.51	−11.63 %	20.40 %	41.46 %
	MED-We	92	25.88	25.28	0.54	22.83	−23.55 %	32.98 %	57.49 %
	ALL	760	18.06	17.92	0.53	12.16	−8.52 %	21.63 %	42.88 %
PM _{2.5}	NEU-We	133	9.70	11.67	0.64	6.33	17.77 %	32.93 %	44.85 %
	NEU-Ce	10	10.96	11.88	0.50	5.31	8.89 %	19.53 %	47.02 %
	MED-We	13	14.39	11.24	0.57	7.68	−32.66 %	35.92 %	51.57 %
	ALL	161	10.41	11.83	0.62	6.53	12.54 %	31.79 %	44.32 %

[Title Page](#)
[Abstract](#)
[Introduction](#)
[Conclusions](#)
[References](#)
[Tables](#)
[Figures](#)
[⏪](#)
[⏩](#)
[◀](#)
[▶](#)
[Back](#)
[Close](#)
[Full Screen / Esc](#)
[Printer-friendly Version](#)
[Interactive Discussion](#)

Contributions to 2012 summertime aerosols in the Euro-Mediterranean region

G. Rea et al.

Table 4. Hourly performance statistics of AOD simulated by CHIMERE (Mod.) during the summer of 2012, together with the observed AOD from AERONET at 500 nm and MODIS at 550 nm (Obs.).

Variable	Region	Number of stations	Number of pairs	Mean		<i>R</i>	RMSE	MFB	MFE
				Obs.	Mod.				
AOD AERONET (500 nm)	NEU-We	17	733	0.16	0.15	0.44	0.11	−1.56 %	42.95 %
	NEU-Ce	5	322	0.23	0.19	0.70	0.10	−14.13 %	35.17 %
	NEU-Ea	6	240	0.19	0.17	0.64	0.08	−11.41 %	30.04 %
	MED-We	25	1694	0.19	0.17	0.73	0.10	−3.52 %	37.47 %
	MED-Ce	7	418	0.22	0.21	0.70	0.08	0.53 %	29.93 %
	MED-Ea	5	438	0.21	0.19	0.65	0.08	−5.17 %	27.95 %
ALL		65	3845	0.19	0.17	0.64	0.10	−4.24 %	36.50 %
AOD MODIS (550 nm)	NEU-We		225	0.19	0.14	0.35	0.07	−29.64 %	36.79 %
	NEU-Ce		58	0.21	0.17	0.70	0.07	−24.91 %	31.66 %
	NEU-Ea		184	0.18	0.17	0.54	0.06	−8.31 %	26.80 %
	MED-We		537	0.30	0.22	0.73	0.10	−32.66 %	33.21 %
	MED-Ce		449	0.22	0.19	0.75	0.04	−12.60 %	17.71 %
	MED-Ea		327	0.25	0.17	0.67	0.10	−39.84 %	39.84 %
	ALL			3380	0.24	0.19	0.62	0.06	−24.60 %

Title Page

Abstract

Introduction

Conclusions

References

Tables

Figures

◀

▶

◀

▶

Back

Close

Full Screen / Esc

Printer-friendly Version

Interactive Discussion

Table 5. Contributions of each emissions source on surface PM_{2.5} and PM₁₀ concentrations and AOD for the full domain and the different sub-regions indicated in Table 1 over the period (1 June to 31 August 2012).

Region	Source	Surface PM _{2.5}		Surface PM ₁₀		AOD	
		µg m ⁻³	%	µg m ⁻³	%	ad.	%
All domain	All sources	13.00		38.28		0.19	
	Anthropogenic	6.76	52.01 %	7.10	18.56 %	0.07	33.95 %
	Fires	0.82	6.27 %	0.92	2.39 %	0.01	5.46 %
	Dust	2.17	16.67 %	23.87	62.35 %	0.05	23.26 %
	Biogenic	1.41	10.83 %	1.43	3.75 %	0.03	14.04 %
	Sea Salt	0.59	4.53 %	2.73	7.12 %	0.0012	0.59 %
NEU-We	All sources	9.46		15.10		0.18	
	Anthropogenic	7.11	75.13 %	7.44	49.28 %	0.10	54.87 %
	Fires	0.12	1.22 %	0.13	0.86 %	0.00	2.20 %
	Dust	0.15	1.62 %	1.18	7.84 %	0.01	4.83 %
	Biogenic	0.68	7.24 %	0.69	4.57 %	0.01	5.01 %
	Sea Salts	0.68	7.19 %	4.33	28.70 %	0.00	1.14 %
NEU-Ce	All sources	11.36		15.86		0.20	
	Anthropogenic	7.16	62.98 %	7.56	47.67 %	0.09	42.65 %
	Fires	0.42	3.66 %	0.45	2.82 %	0.01	4.62 %
	Dust	0.52	4.58 %	3.45	21.78 %	0.02	9.97 %
	Biogenic	2.48	21.83 %	2.51	15.82 %	0.04	21.51 %
	Sea Salts	0.16	1.42 %	0.58	3.68 %	0.00	0.43 %
NEU-Ea	All sources	9.78		13.24		0.19	
	Anthropogenic	4.91	50.14 %	5.30	40.00 %	0.06	33.99 %
	Fires	0.72	7.31 %	0.75	5.64 %	0.01	7.26 %
	Dust	0.35	3.57 %	2.28	17.19 %	0.02	7.95 %
	Biogenic	1.51	15.45 %	1.53	11.57 %	0.04	22.01 %
	Sea Salts	0.12	1.27 %	0.43	3.27 %	0.00	0.26 %
MED-We	All sources	15.15		88.17		0.23	
	Anthropogenic	4.92	32.50 %	5.17	5.86 %	0.04	18.72 %
	Fires	0.83	5.45 %	0.95	1.08 %	0.01	4.51 %
	Dust	6.54	43.19 %	75.63	85.78 %	0.11	49.20 %
	Biogenic	0.82	5.38 %	0.84	0.95 %	0.02	7.12 %
	Sea Salts	0.62	4.12 %	2.96	3.36 %	0.00	0.58 %
MED-Ce	All sources	15.66		33.22		0.20	
	Anthropogenic	8.54	54.55 %	8.89	26.77 %	0.06	31.50 %
	Fires	1.91	12.22 %	2.16	6.51 %	0.02	9.82 %
	Dust	1.36	8.66 %	14.39	43.31 %	0.04	22.64 %
	Biogenic	1.84	11.77 %	1.90	5.70 %	0.03	16.75 %
	Sea Salts	0.90	5.75 %	3.60	10.83 %	0.00	0.57 %
MED-Ea	All sources	12.90		22.90		0.17	
	Anthropogenic	7.83	60.67 %	8.24	35.98 %	0.07	41.01 %
	Fires	0.45	3.48 %	0.50	2.20 %	0.01	3.81 %
	Dust	0.78	6.06 %	7.09	30.98 %	0.02	10.88 %
	Biogenic	1.42	11.02 %	1.45	6.34 %	0.03	18.64 %
	Sea Salts	0.67	5.17 %	2.84	12.40 %	0.00	0.46 %

Contributions to 2012 summertime aerosols in the Euro-Mediterranean region

G. Rea et al.

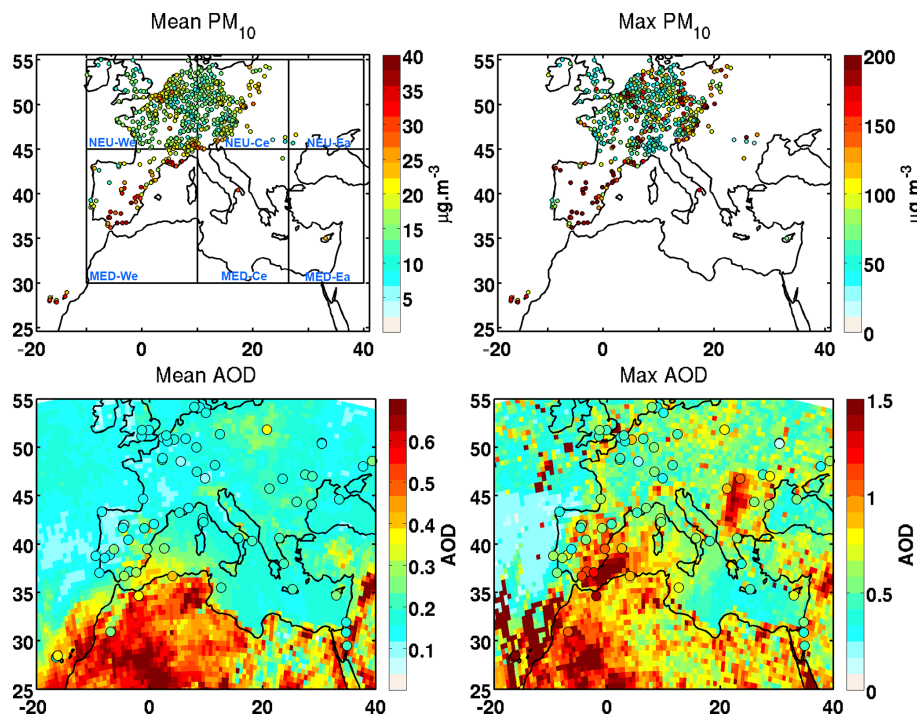


Figure 1. Summer 2012 (1 June to 31 August) daily average for surface PM_{10} concentrations from the AirBase network (upper left) and Aerosol Optical Depth at 550 and 500 nm respectively from MODIS instrument and AERONET stations (bottom left). Daily maximum over the period is shown on upper right panel for surface PM_{10} concentrations and bottom right panel for Aerosol Optical Depth.

Title Page

Abstract

Introduction

Conclusions

References

Tables

Figures

◀

▶

◀

▶

Back

Close

Full Screen / Esc

Printer-friendly Version

Interactive Discussion

**Contributions to 2012
summertime aerosols
in the
Euro-Mediterranean
region**

G. Rea et al.

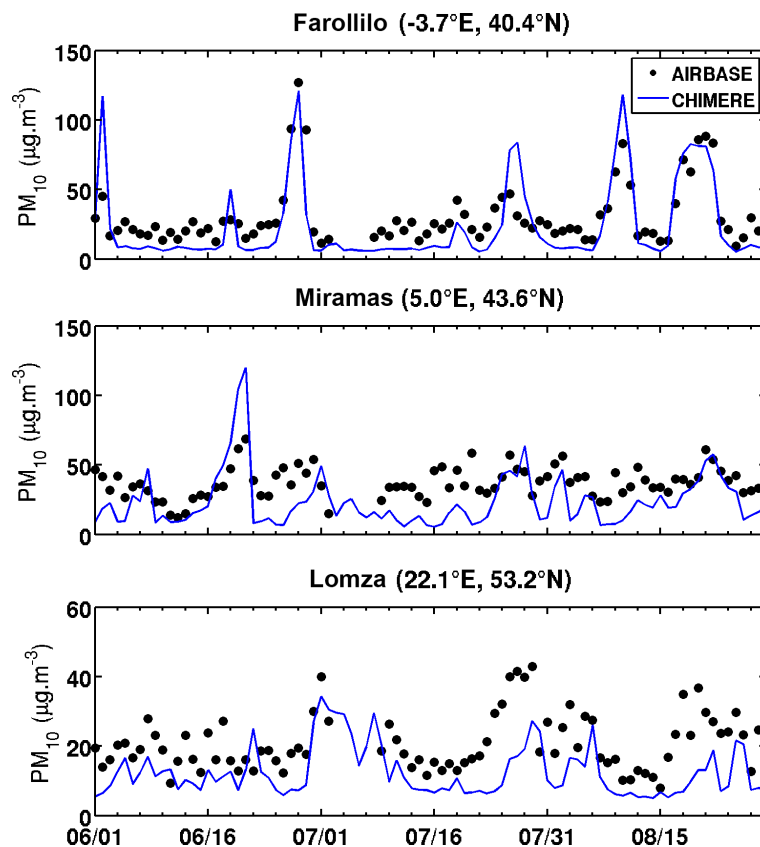


Figure 2. Time series from 1 June to 31 August of daily mean surface PM_{10} concentrations from 3 stations of the AirBase network. First station is located near Salamanca in Spain, second is in Miramas in South of France, and third is in Lomza in Poland. The corresponding simulated CHIMERE concentrations (spatially co-localized) are also indicated (blue line).

[Title Page](#)[Abstract](#)[Introduction](#)[Conclusions](#)[References](#)[Tables](#)[Figures](#)[◀](#)[▶](#)[◀](#)[▶](#)[Back](#)[Close](#)[Full Screen / Esc](#)[Printer-friendly Version](#)[Interactive Discussion](#)

**Contributions to 2012
summertime aerosols
in the
Euro-Mediterranean
region**

G. Rea et al.

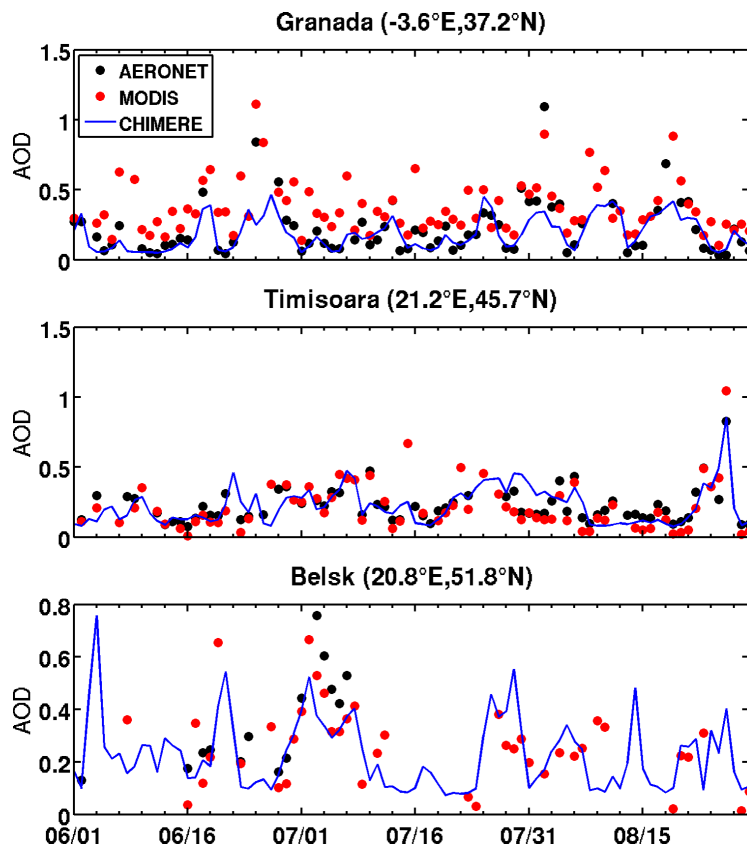


Figure 3. Time series from 1 June to 31 August of the daily AOD at 500 nm from three AERONET stations. First station is Granada in Spain, second is Timisoara in Romania, and third is Belsk in Poland. Values from MODIS at 550 nm are also indicated in red dots at these stations, as well as the simulated spatially co-localized 550 nm AOD from CHIMERE (blue line).

[Title Page](#)[Abstract](#)[Introduction](#)[Conclusions](#)[References](#)[Tables](#)[Figures](#)[◀](#)[▶](#)[◀](#)[▶](#)[Back](#)[Close](#)[Full Screen / Esc](#)[Printer-friendly Version](#)[Interactive Discussion](#)

Contributions to 2012 summertime aerosols in the Euro-Mediterranean region

G. Rea et al.

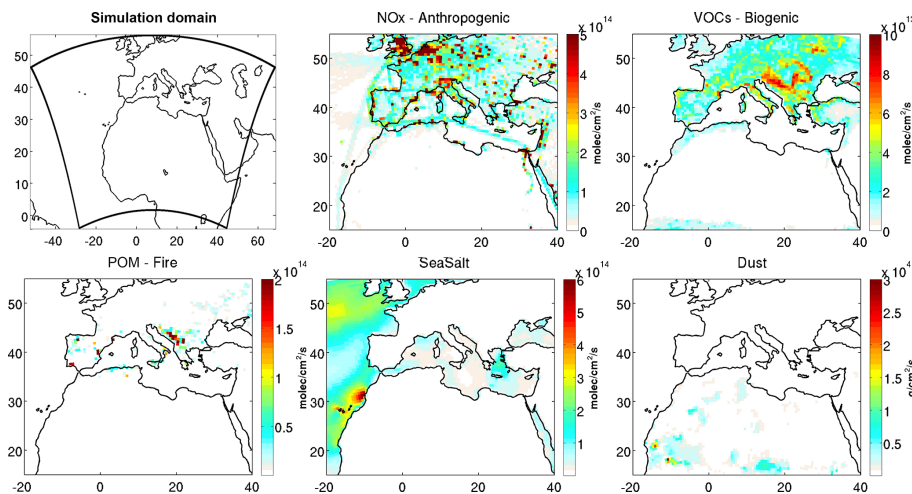


Figure 4. Total fluxes of different aerosol precursors or primary aerosol from each source during the summer of 2012: anthropogenic emissions of nitrogen oxides (NO_x), biogenic emissions of volatile organic compounds (VOCs), fire emissions of primary organic matter (POM), mineral dust and sea salt emissions.

Title Page

Abstract

Introduction

Conclusions

References

Tables

Figures

◀

▶

◀

▶

Back

Close

Full Screen / Esc

Printer-friendly Version

Interactive Discussion

Contributions to 2012 summertime aerosols in the Euro-Mediterranean region

G. Rea et al.

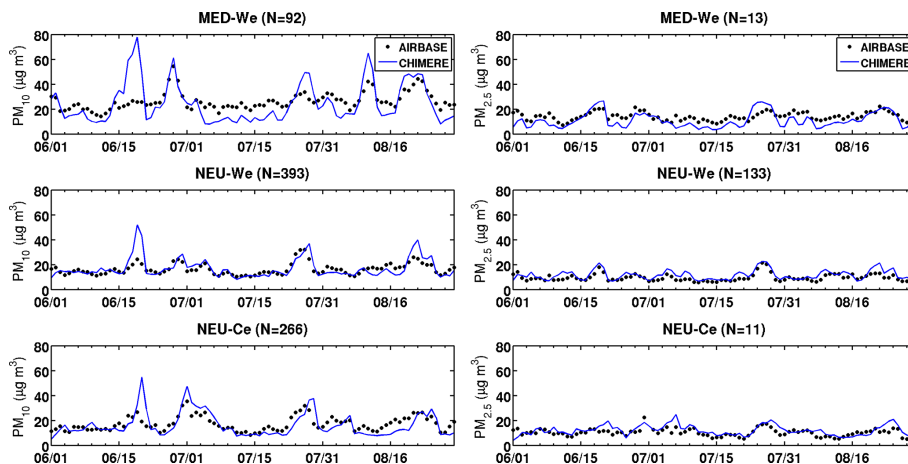


Figure 5. Temporal evolution during the Summer of 2012 of observed surface PM_{10} (left column) and surface $PM_{2.5}$ (right column) concentrations at AirBase stations (number in each region indicated by the value of N), in addition to corresponding and collocated simulated surface concentration from CHIMERE (blue line).

Title Page

Abstract

Introduction

Conclusions

References

Tables

Figures

◀

▶

◀

▶

Back

Close

Full Screen / Esc

Printer-friendly Version

Interactive Discussion

Contributions to 2012 summertime aerosols in the Euro-Mediterranean region

G. Rea et al.

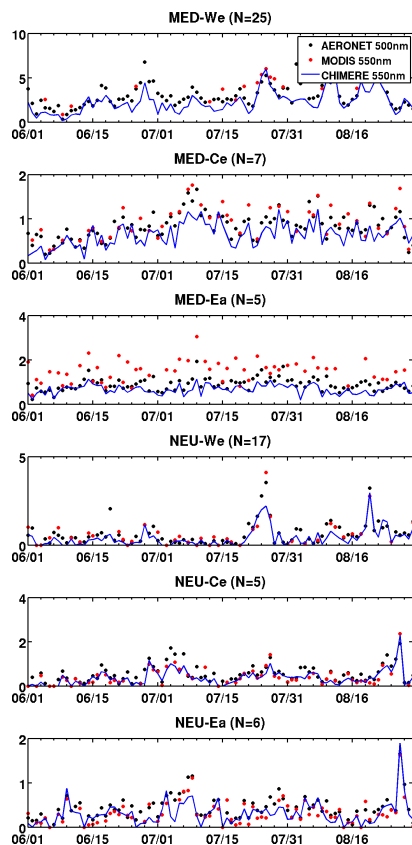


Figure 6. Temporal evolution of the daily mean AOD observed at 500 nm at the AERONET stations (black dots) and at 550 nm from MODIS Aerosol Products (red dots), in addition to simulated AOD at 550 nm by the CHIMERE model (blue line) during the Summer of 2012. Number of stations in each region is indicated by the value of N .

[Title Page](#)[Abstract](#)[Introduction](#)[Conclusions](#)[References](#)[Tables](#)[Figures](#)[◀](#)[▶](#)[◀](#)[▶](#)[Back](#)[Close](#)[Full Screen / Esc](#)[Printer-friendly Version](#)[Interactive Discussion](#)

Contributions to 2012 summertime aerosols in the Euro-Mediterranean region

G. Rea et al.

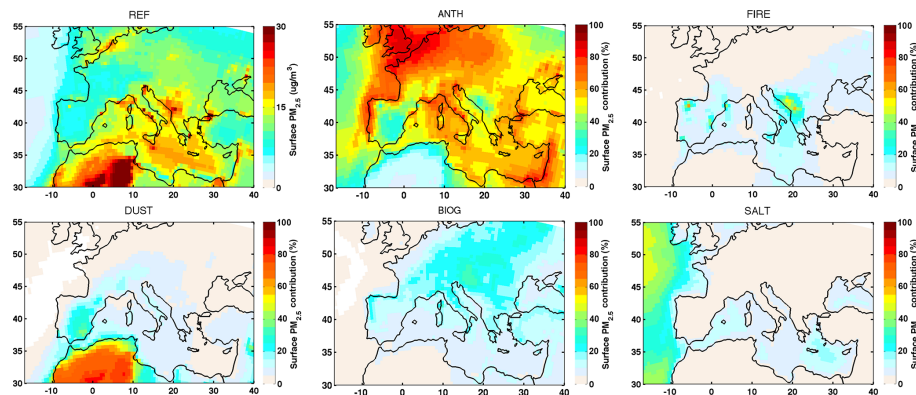


Figure 7. Relative contribution of each source (i.e. the baseline simulation minus the sensitivity simulation where the respective source has been eliminated) to the simulated surface $\text{PM}_{2.5}$, averaged over the period (1 June to 31 August 2012). The first plot represents the reference surface concentration over the same period.

[Title Page](#)[Abstract](#)[Introduction](#)[Conclusions](#)[References](#)[Tables](#)[Figures](#)[◀](#)[▶](#)[◀](#)[▶](#)[Back](#)[Close](#)[Full Screen / Esc](#)[Printer-friendly Version](#)[Interactive Discussion](#)

Contributions to 2012 summertime aerosols in the Euro-Mediterranean region

G. Rea et al.

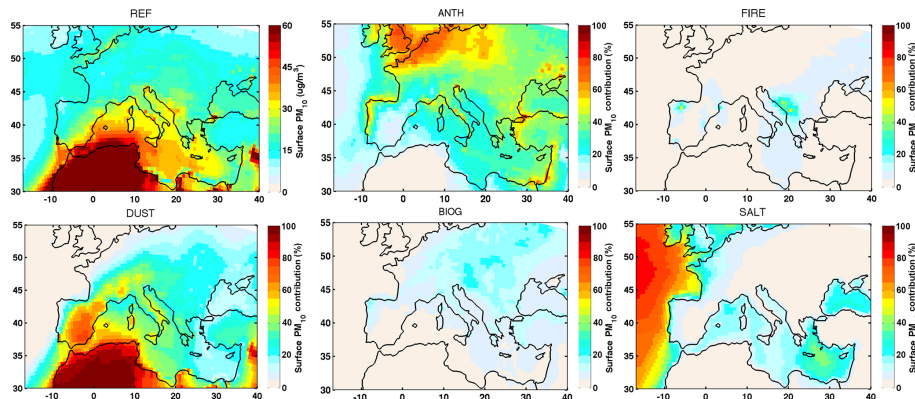


Figure 8. Relative contribution of each source (i.e. the baseline simulation minus the sensitivity simulation where the respective source has been eliminated) to the simulated surface PM_{10} , averaged over the period (1 June to 31 August 2012). The first plot represents the reference surface concentration over the same period.

Title Page

Abstract

Introduction

Conclusions

References

Tables

Figures

◀

▶

◀

▶

Back

Close

Full Screen / Esc

Printer-friendly Version

Interactive Discussion

Contributions to 2012 summertime aerosols in the Euro-Mediterranean region

G. Rea et al.

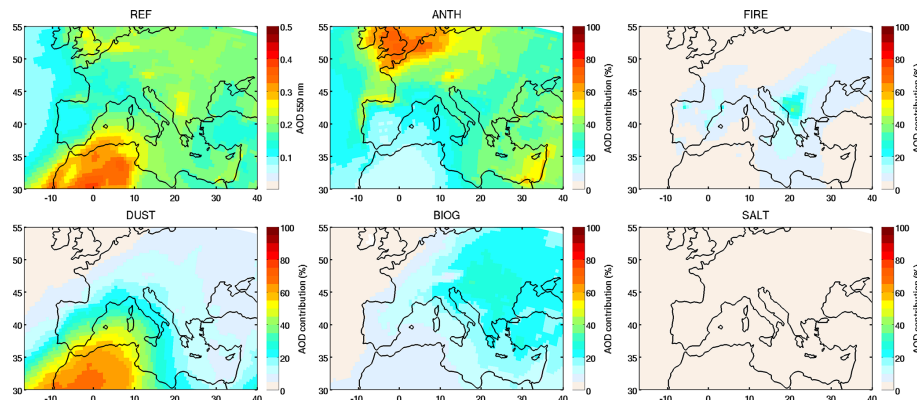


Figure 9. Relative contribution of each source (i.e. the baseline simulation minus the sensitivity simulation where the respective source has been eliminated) to the simulated AOD at 550 nm, averaged over the period (1 June to 31 August 2012). The first plot represents the reference simulation of AOD over the same period.

[Title Page](#)[Abstract](#)[Introduction](#)[Conclusions](#)[References](#)[Tables](#)[Figures](#)[◀](#)[▶](#)[◀](#)[▶](#)[Back](#)[Close](#)[Full Screen / Esc](#)[Printer-friendly Version](#)[Interactive Discussion](#)

Contributions to 2012 summertime aerosols in the Euro-Mediterranean region

G. Rea et al.

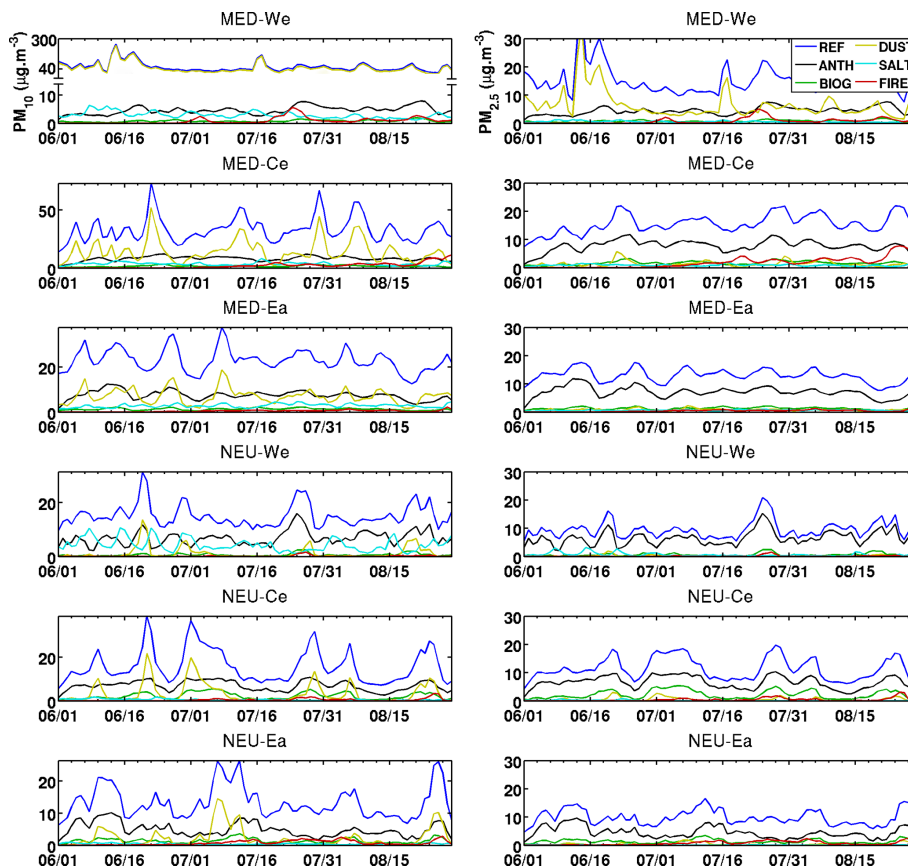


Figure 10. Temporal evolution during the Summer of 2012 (1 June to 31 August 2012) of the total simulated surface PM_{10} (left column) and surface $PM_{2.5}$ (right column) concentrations and the contributions from each source (i.e. the baseline simulation minus the sensitivity simulation where the respective source has been eliminated), averaged within each sub-region indicated in Table 1.

Contributions to 2012 summertime aerosols in the Euro-Mediterranean region

G. Rea et al.

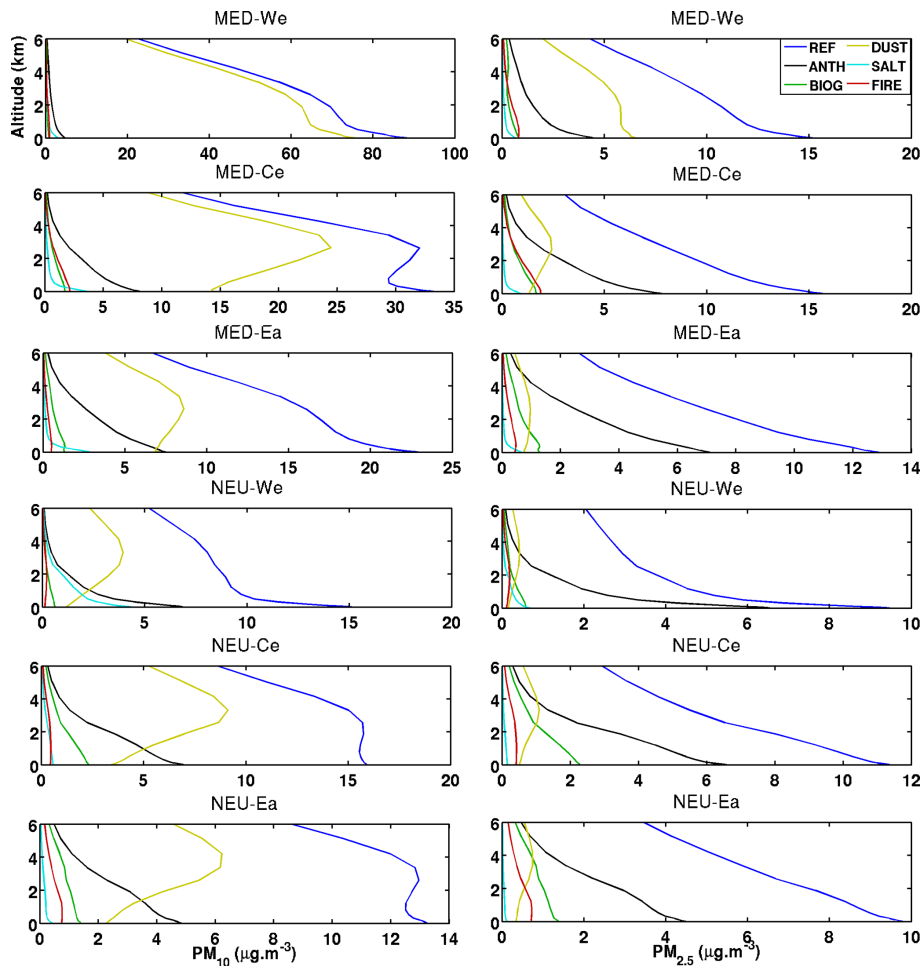


Figure 11. Mean vertical profiles of PM_{10} (left column) and $PM_{2.5}$ (right column) for each sub-region indicated in Table 1 and for each contributions.

Title Page

Abstract

Introduction

Conclusions

References

Tables

Figures

◀

▶

◀

▶

Back

Close

Full Screen / Esc

Printer-friendly Version

Interactive Discussion



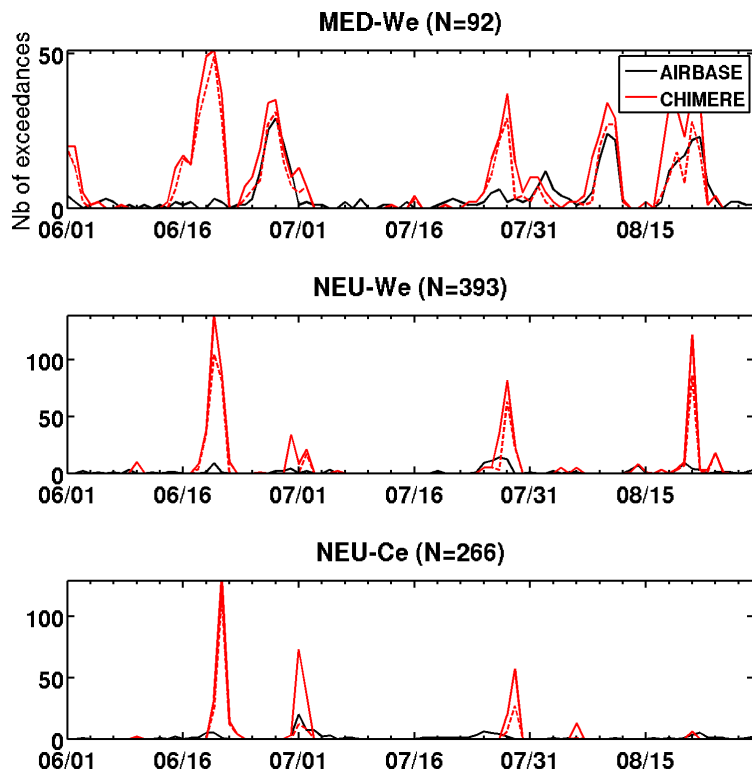


Figure 12. Number of stations in daily exceedances of the European Union air quality threshold of $50 \mu\text{g m}^{-3}$ for daily mean PM_{10} concentrations during the Summer of 2012 (1 June to 31 August), as observed at the rural and background AirBase stations (black line) and simulated by the CHIMERE model at the same locations (red line). The red dashed line corresponds to the simulated number of stations in daily exceedances when the threshold is set to respectively 75, 58 and $62 \mu\text{g m}^{-3}$ for MED-We, NEU-We and NEU-Ce, when the contribution of mineral dust is more than 60% of the total concentration.

Contributions to 2012 summertime aerosols in the Euro-Mediterranean region

G. Rea et al.

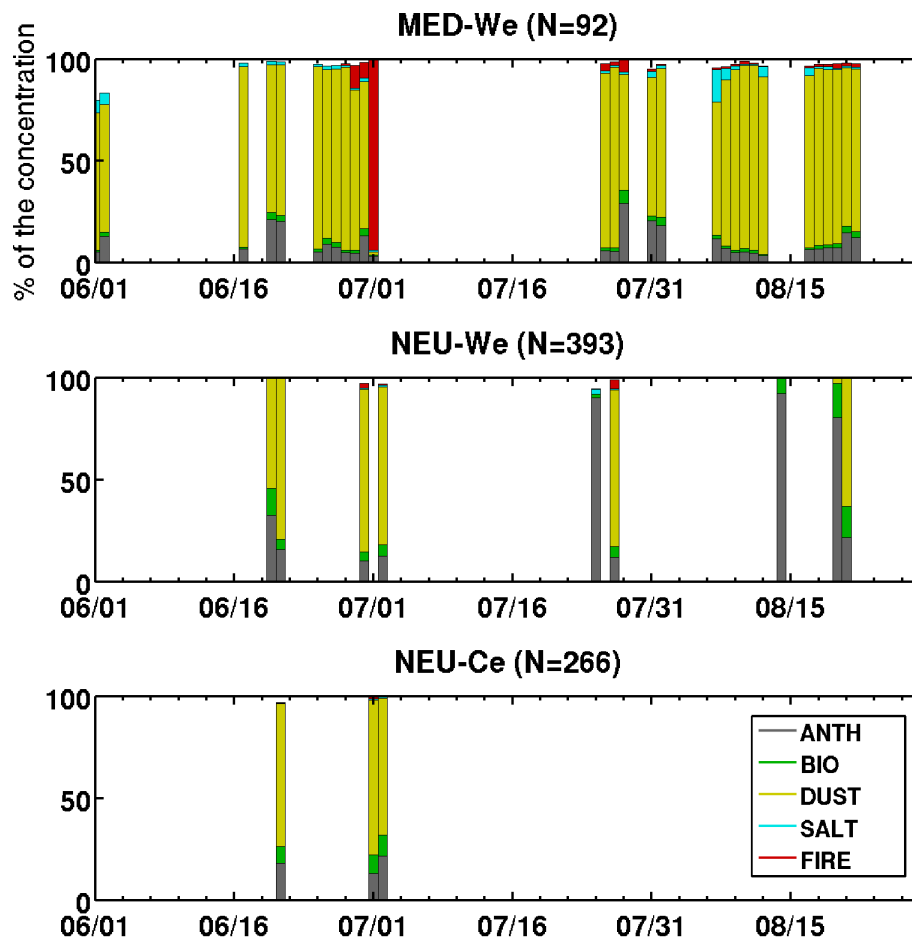


Figure 13. Simulated relative contribution of each source to surface PM_{10} concentration during the Summer of 2012 (1 June to 31 August), on average when exceedances of the daily air quality threshold are detected by both observations and model at the same time and location.

Title Page

Abstract

Introduction

Conclusions

References

Tables

Figures

◀

▶

◀

▶

Back

Close

Full Screen / Esc

Printer-friendly Version

Interactive Discussion

